

# PAMAM-calix-dendrimers: Synthesis and Thiacalixarene Conformation Effect on DNA Binding

Olga Mostovaya<sup>1</sup>, Pavel Padnya<sup>1,\*</sup>, Igor Shiabiev<sup>1</sup>, Timur Mukhametzyanov<sup>1</sup> and Ivan Stoikov<sup>1,\*</sup>

1. NMR, IR and mass spectra of synthesized compounds .....	2
2. Complexation investigation .....	14
2.1 UV-Vis spectra .....	14
2.2 Fluorescence spectra .....	20
2.3 CD spectra .....	24
2.4 DLS data .....	25
2.5 TEM images .....	36

## 1. NMR, IR and mass spectra of synthesized compounds

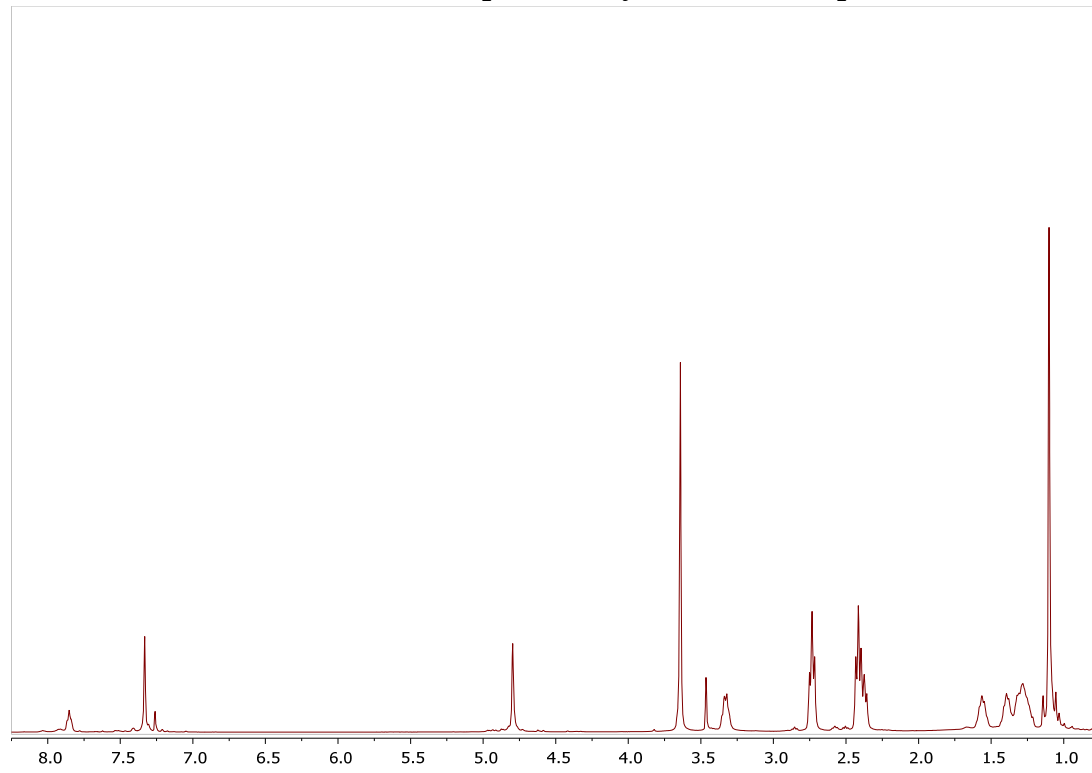


Fig. S1. <sup>1</sup>H NMR spectrum of **G0.5-cone**, CDCl<sub>3</sub>, 298 K, 400 MHz

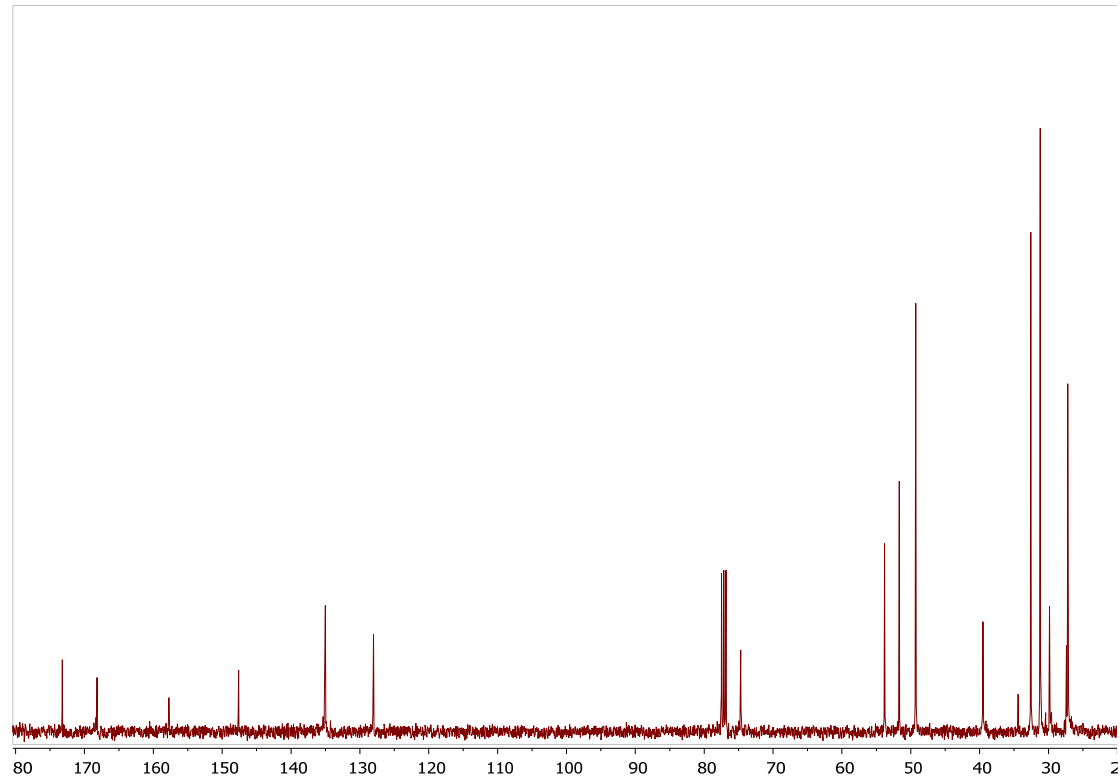


Fig. S2. <sup>13</sup>C{<sup>1</sup>H} NMR spectrum of **G0.5-cone**, CDCl<sub>3</sub>, 298 K, 100 MHz

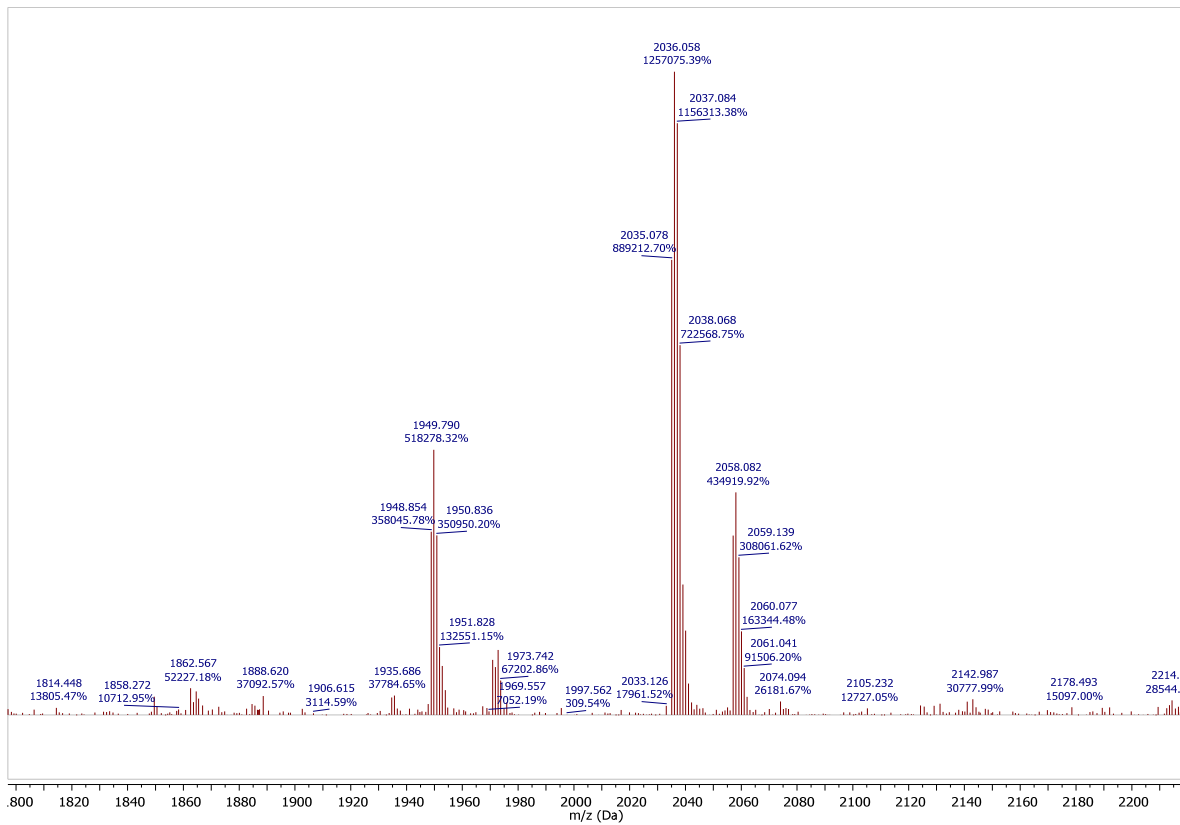


Fig. S3. Mass spectrum (MALDI TOF, 4-nitroaniline matrix) of G0.5-cone

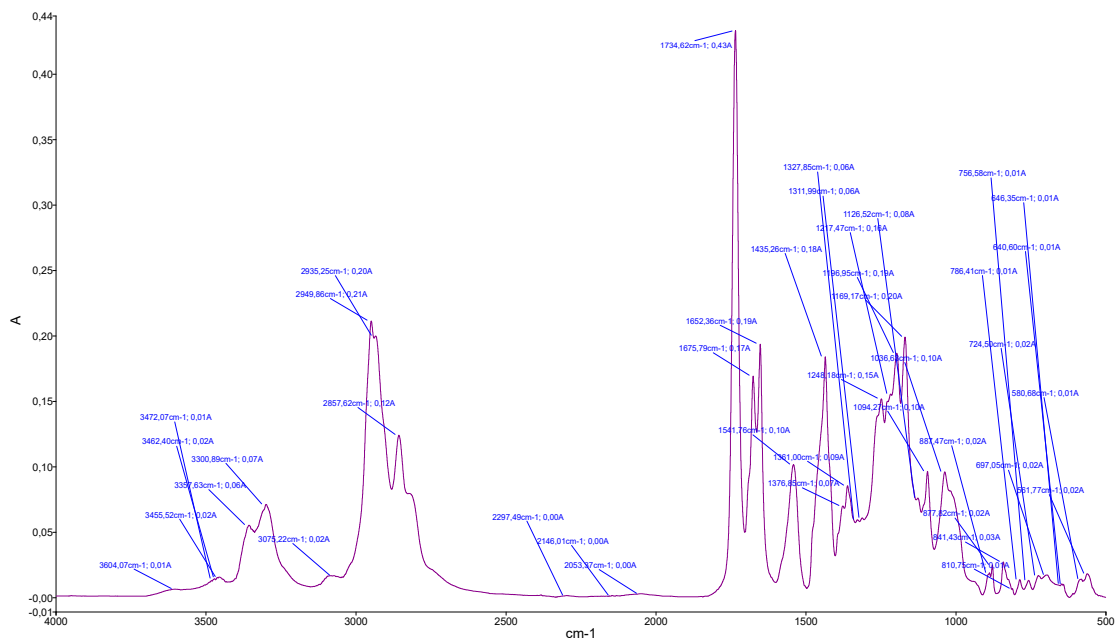


Fig. S4. FTIR-ATR spectrum of G0.5-cone

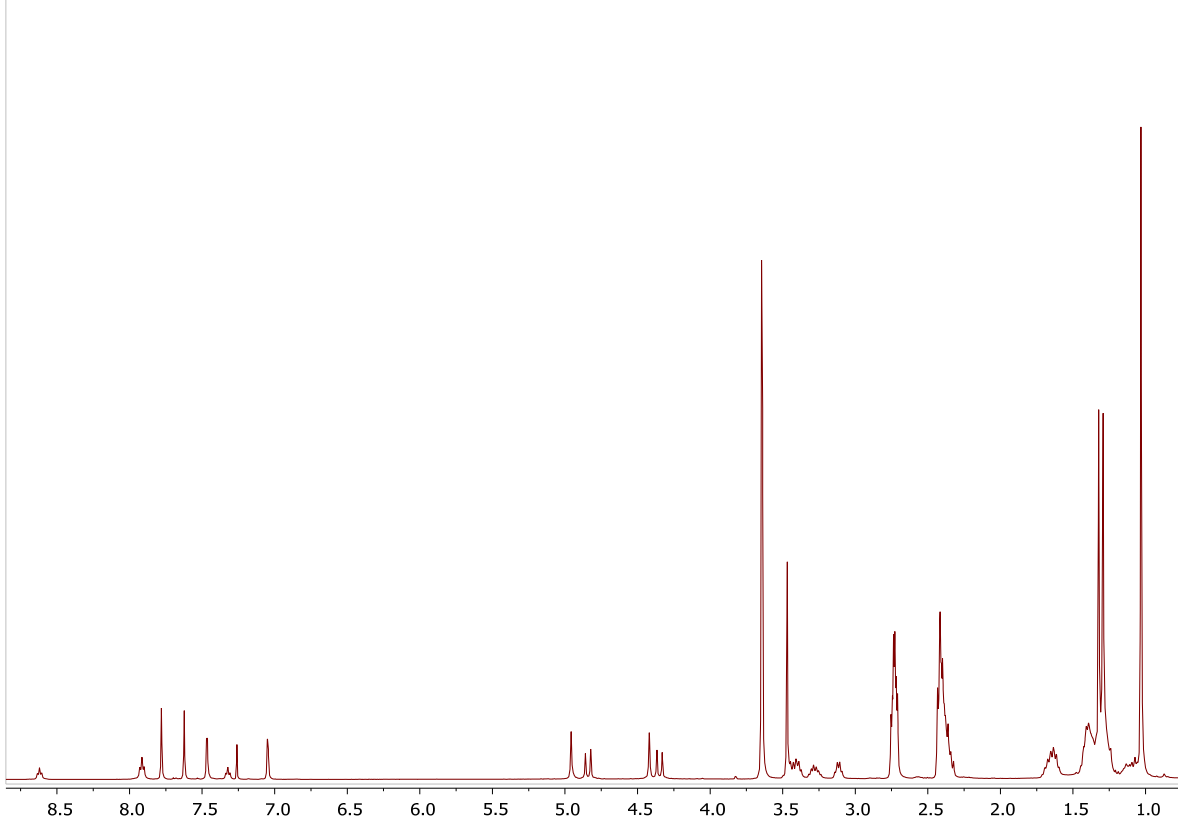


Fig. S5. <sup>1</sup>H NMR spectrum of **G0.5-paco**,  $\text{CDCl}_3$ , 298 K, 400 MHz

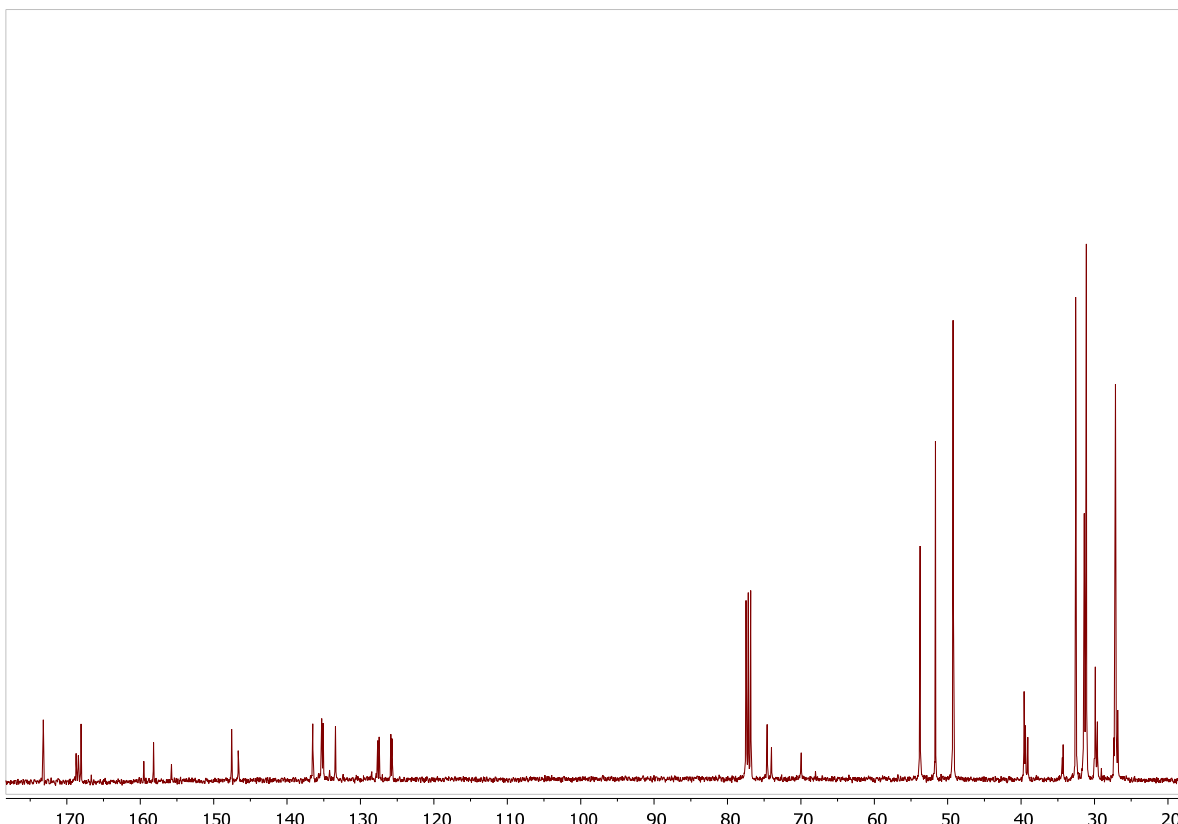


Fig. S6. <sup>13</sup>C{<sup>1</sup>H} NMR spectrum of **G0.5-paco**,  $\text{CDCl}_3$ , 298 K, 100 MHz

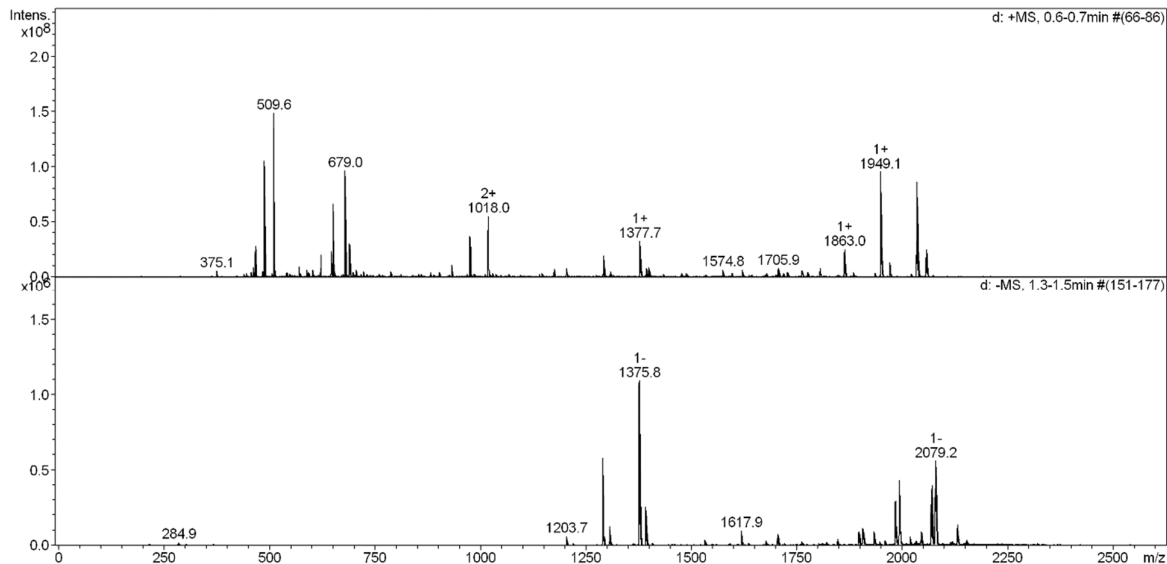


Fig. S7. Mass spectrum (ESI) of G0.5-paco

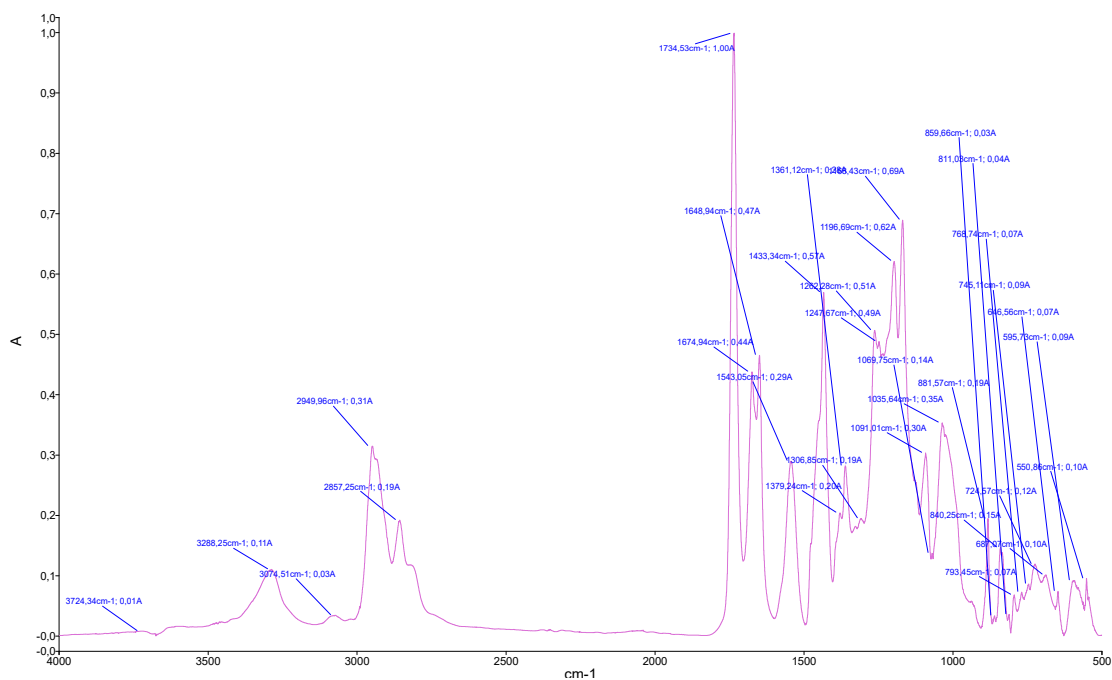


Fig. S8. FTIR-ATR spectrum of G0.5-paco

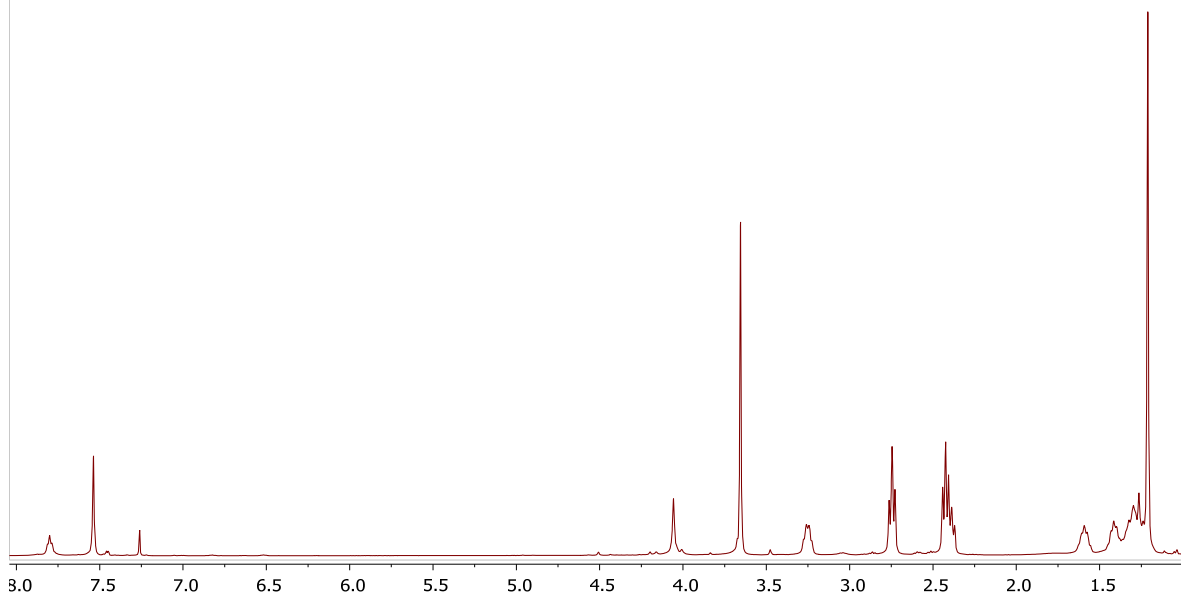


Fig. S9. <sup>1</sup>H NMR spectrum of **G0.5-alt**, CDCl<sub>3</sub>, 298 K, 400 MHz

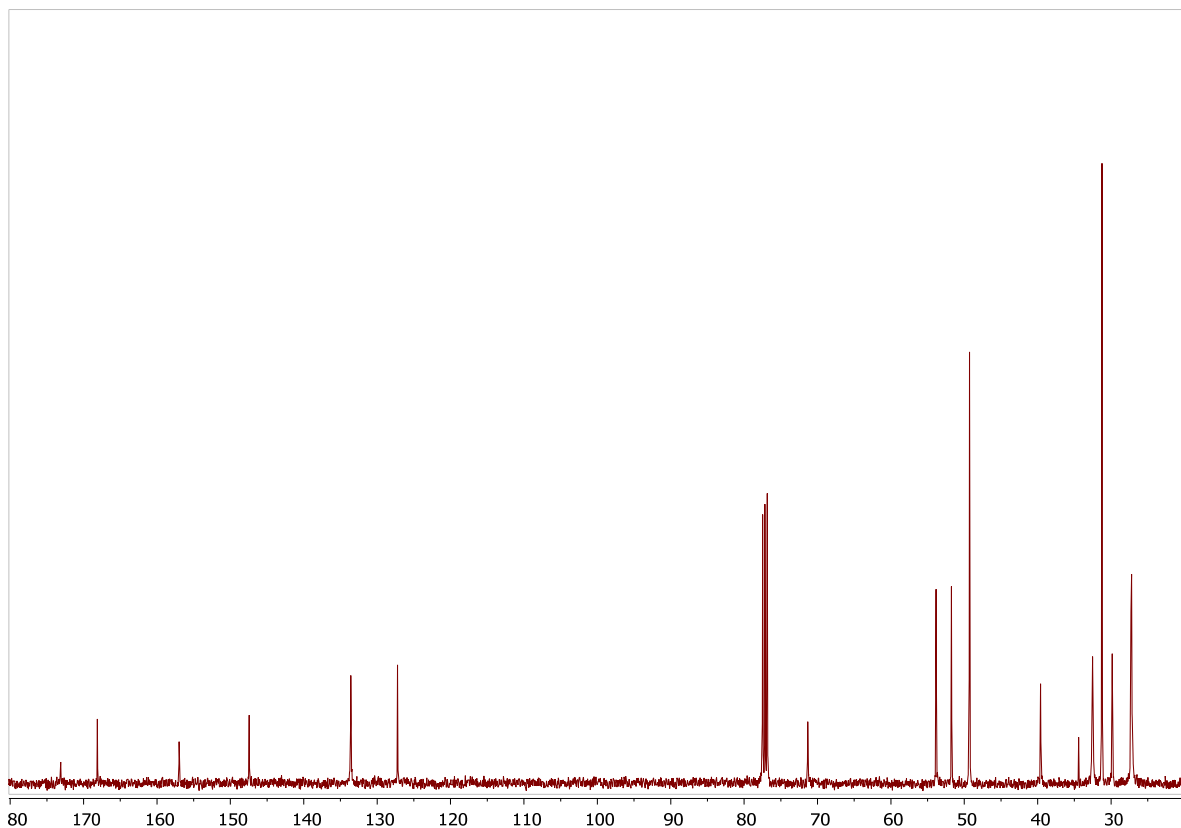


Fig. S10. <sup>13</sup>C{<sup>1</sup>H} NMR spectrum of **G0.5-alt**, CDCl<sub>3</sub>, 298 K, 100 MHz

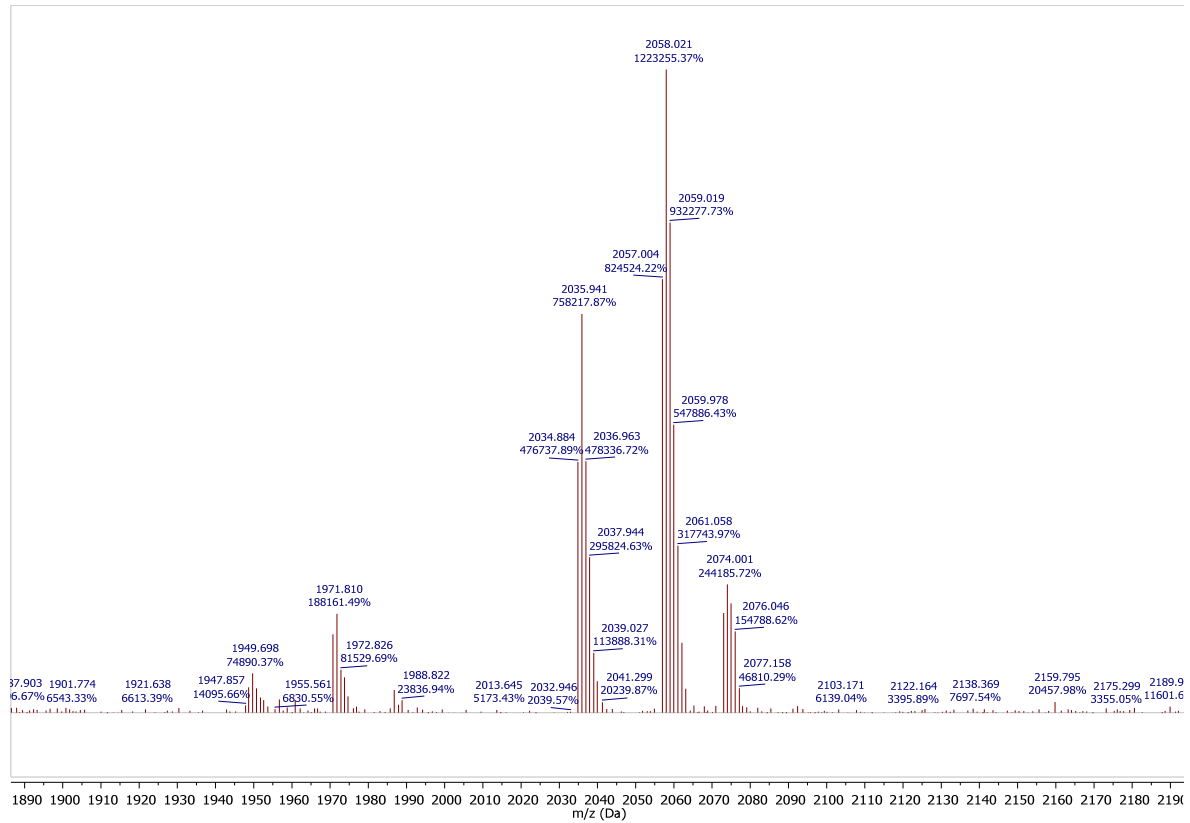


Fig. S11. Mass spectrum (MALDI TOF, 4-nitroaniline matrix) of G0.5-alt

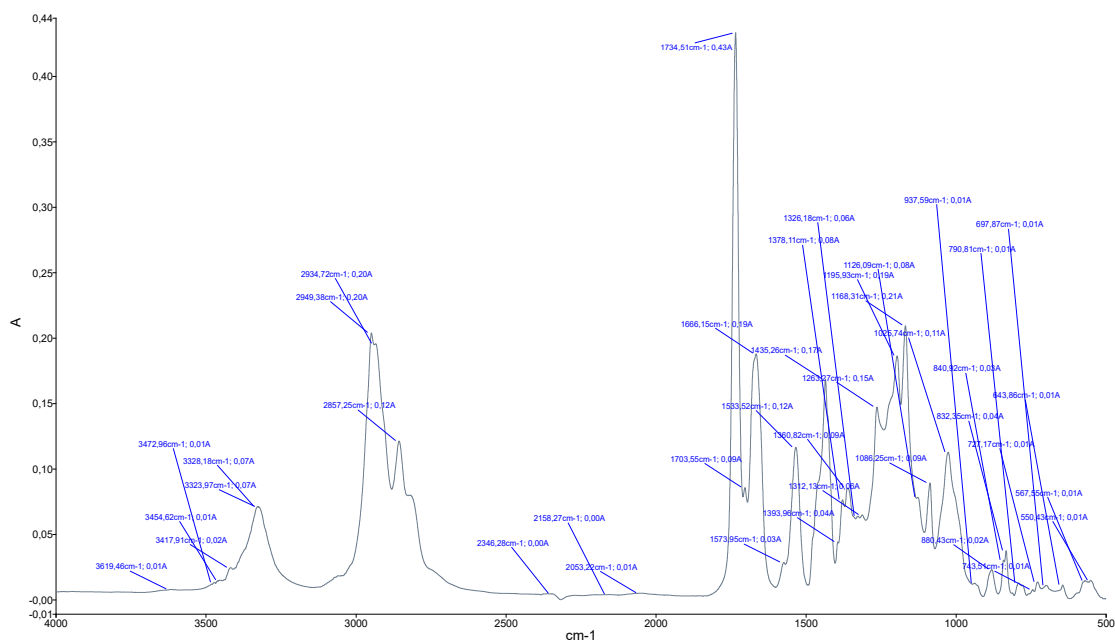


Fig. S12. FTIR-ATR spectrum of G0.5-alt

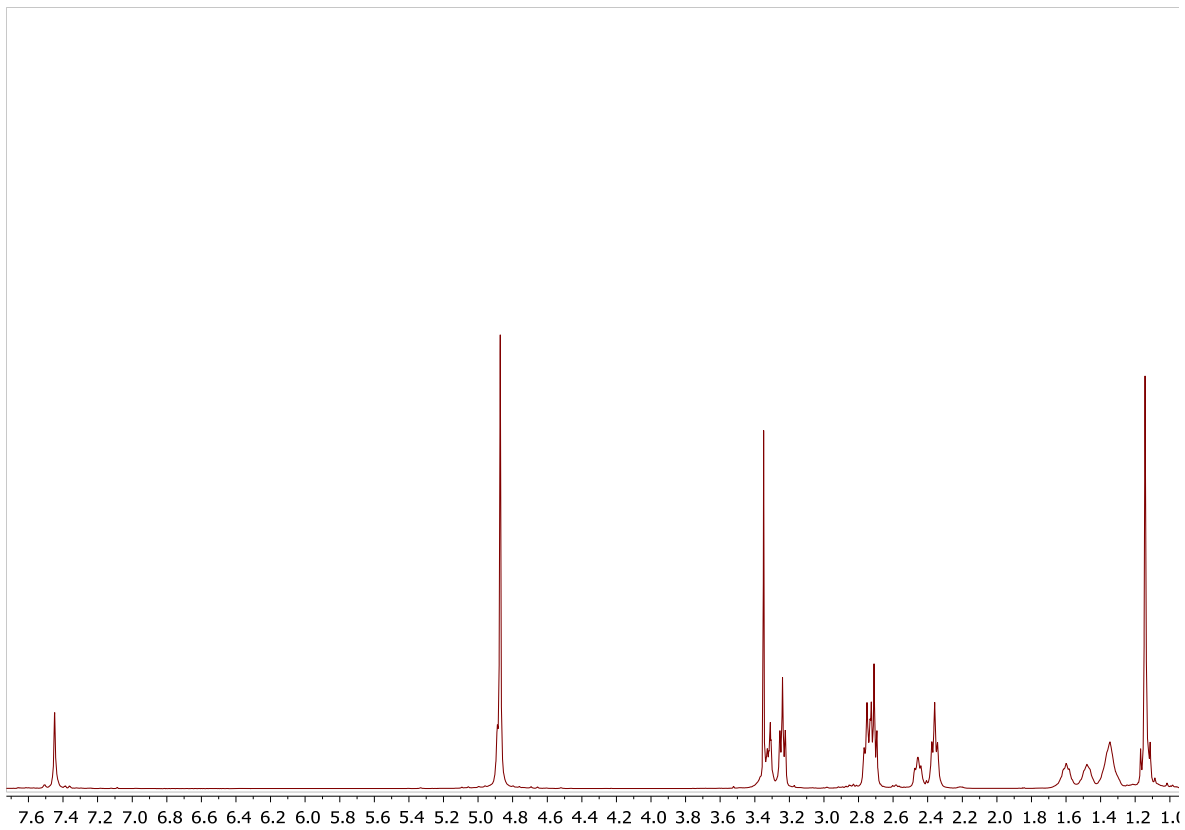


Fig. S13.  $^1\text{H}$  NMR spectrum of **G1-cone**,  $\text{CD}_3\text{OD}$ , 298 K, 400 MHz

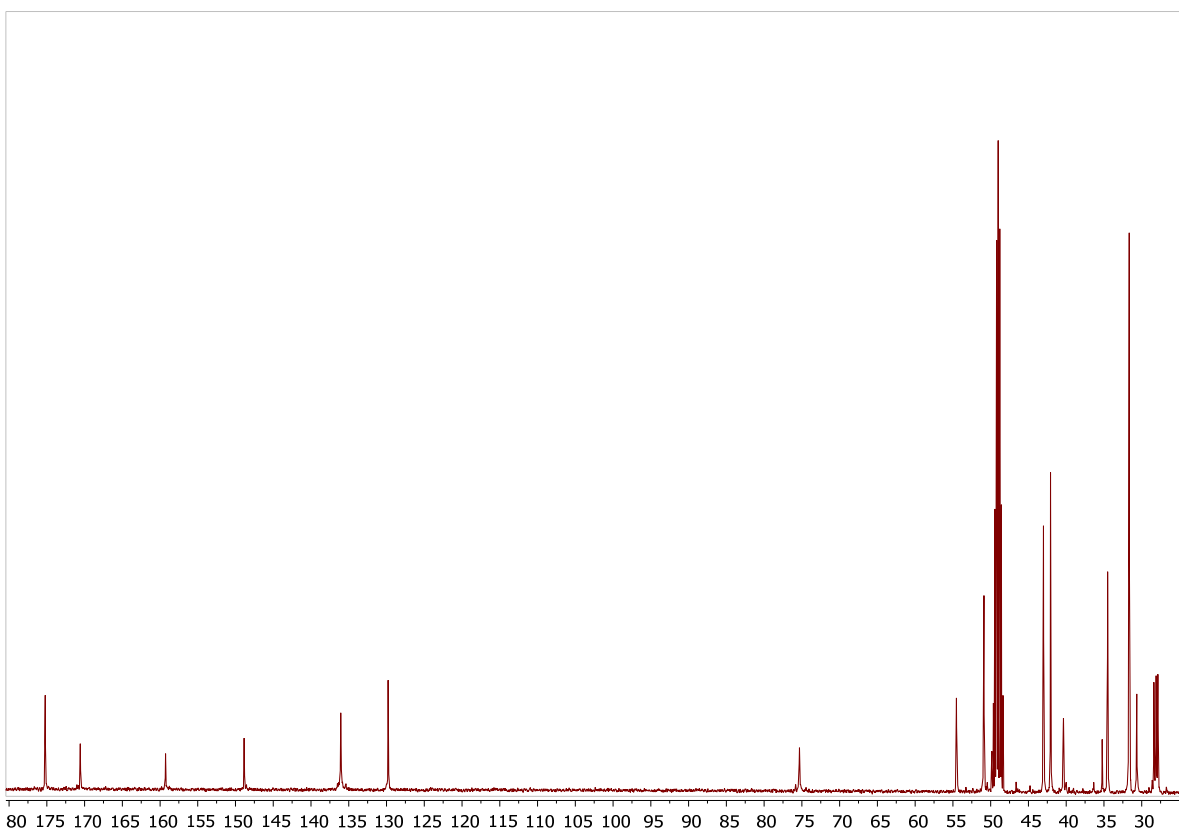


Fig. S14.  $^{13}\text{C}\{\text{H}\}$  NMR spectrum of **G1-cone**,  $\text{CD}_3\text{OD}$ , 298 K, 100 MHz

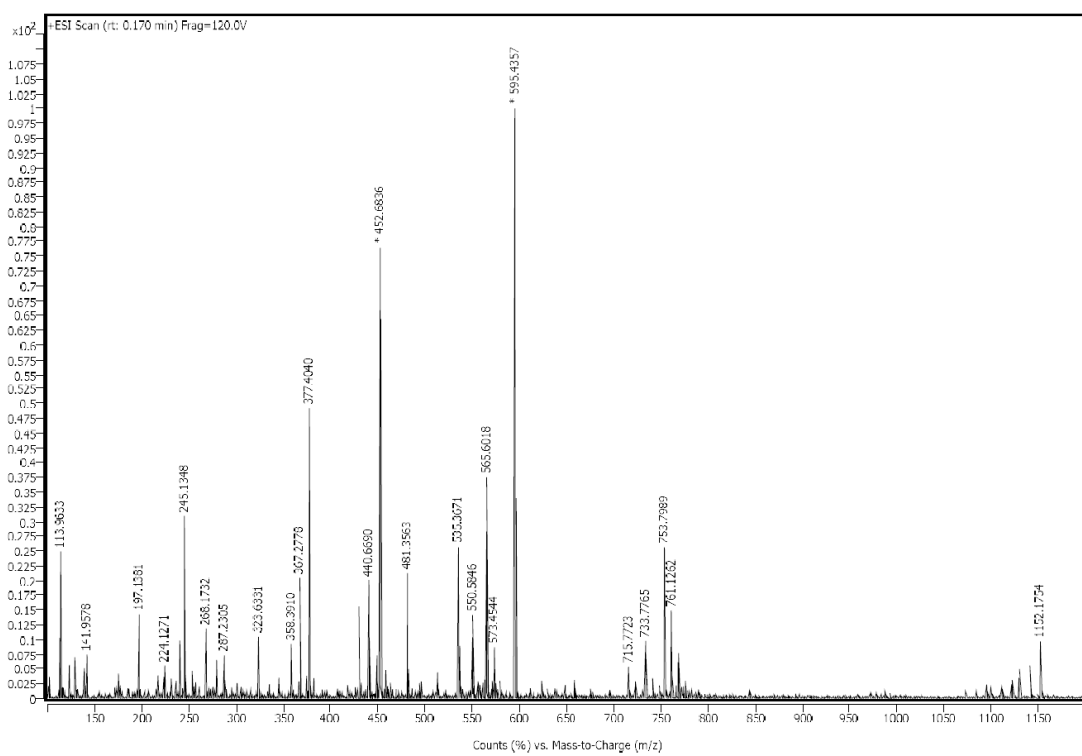


Fig. S15. Mass spectrum (HRESI) of G1-cone

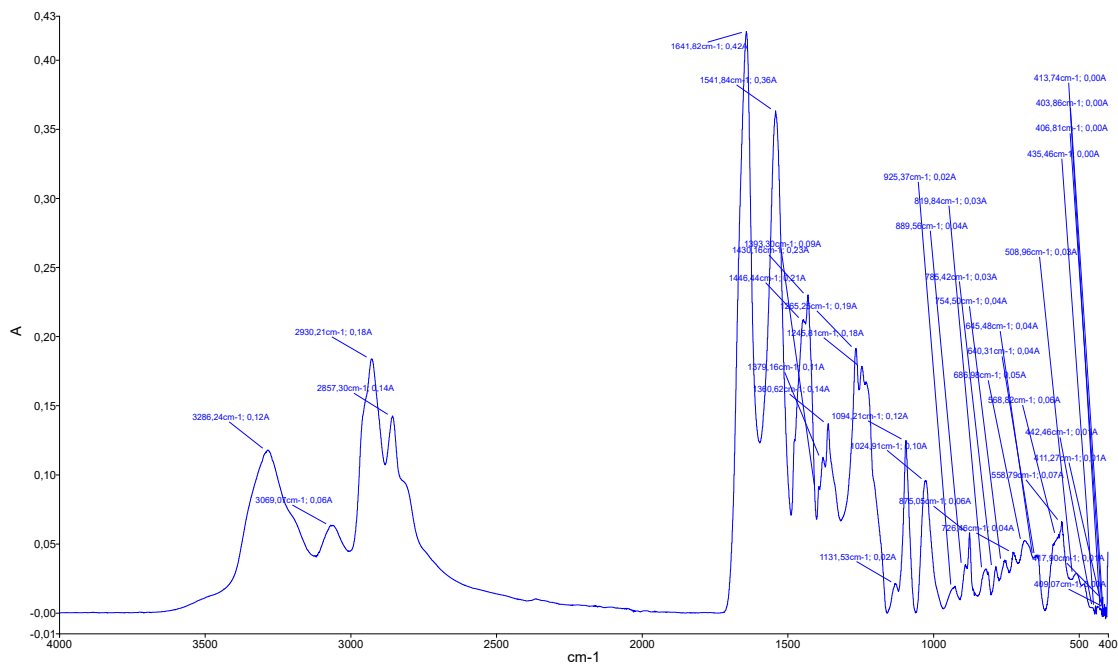


Fig. S16. FTIR-ATR spectrum of G1-cone

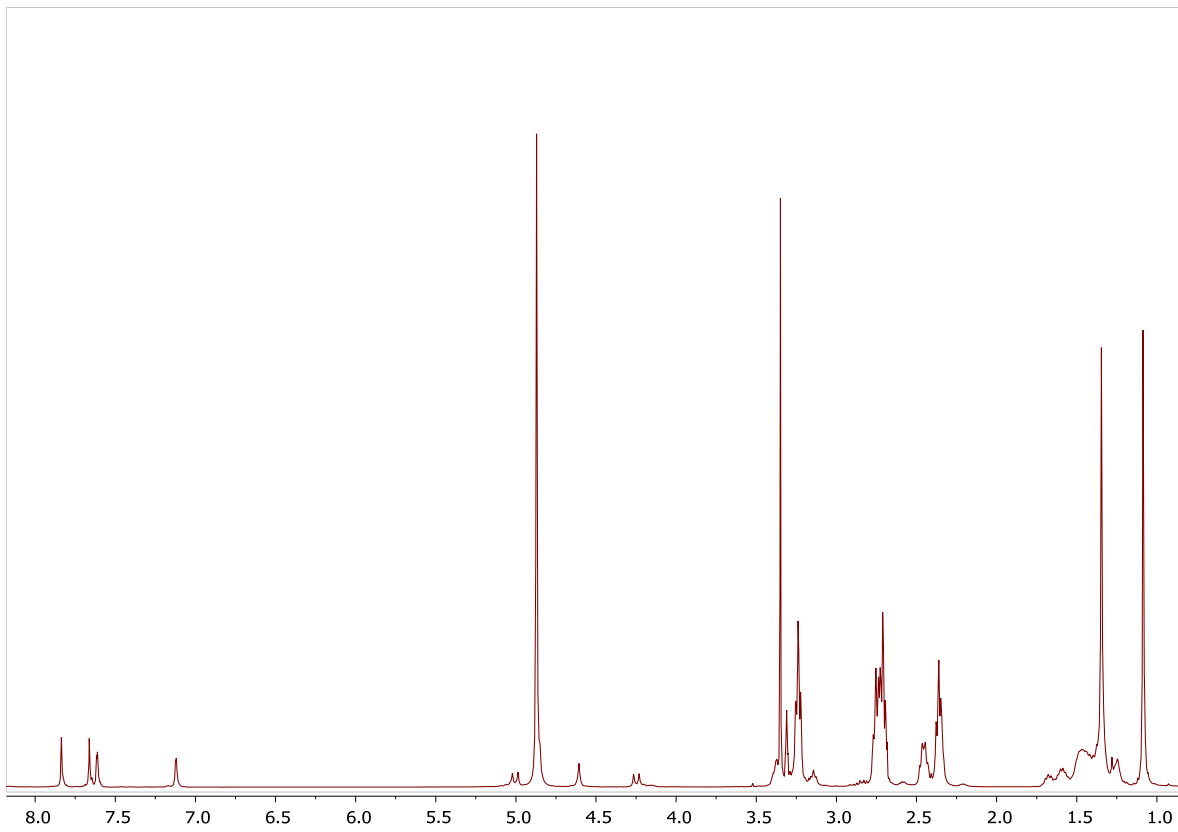


Fig. S17.  $^1\text{H}$  NMR spectrum of **G1-paco**,  $\text{CD}_3\text{OD}$ , 298 K, 400 MHz

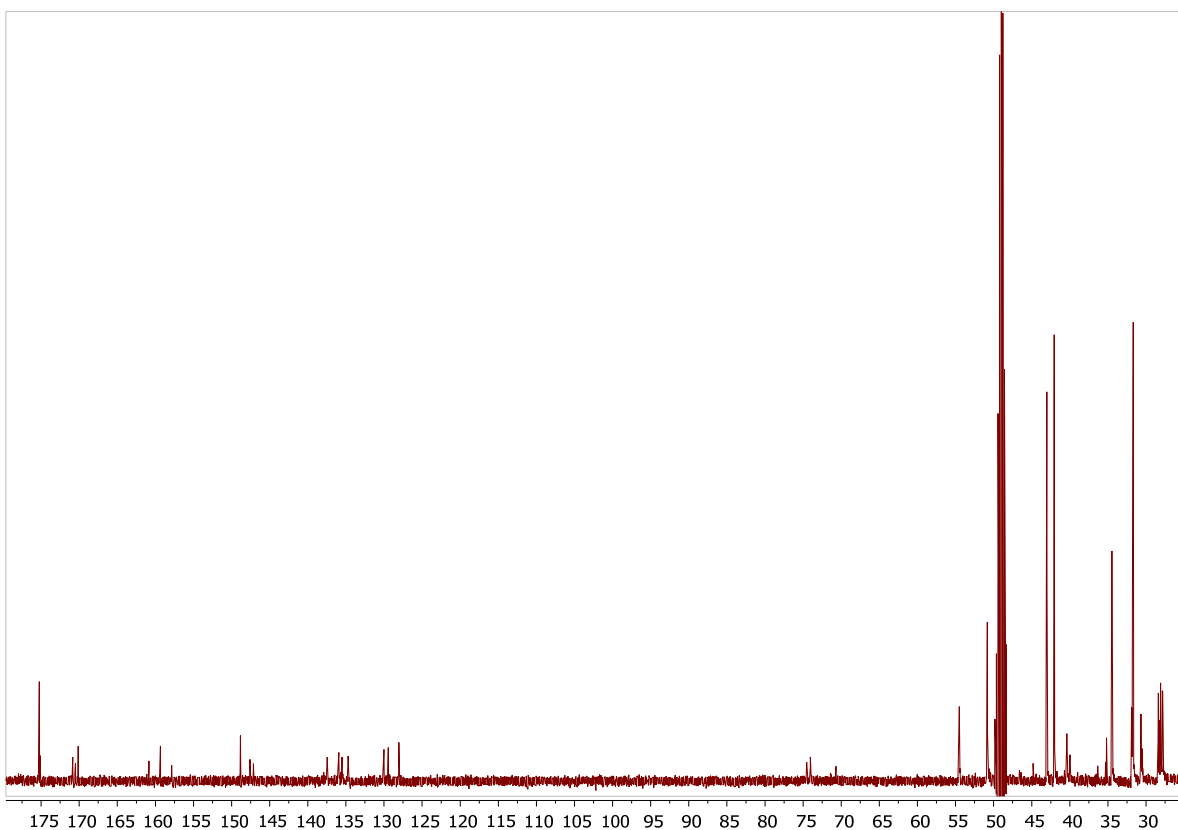


Fig. S18.  $^{13}\text{C}\{\text{H}\}$  NMR spectrum of **G1-paco**,  $\text{CD}_3\text{OD}$ , 298 K, 100 MHz

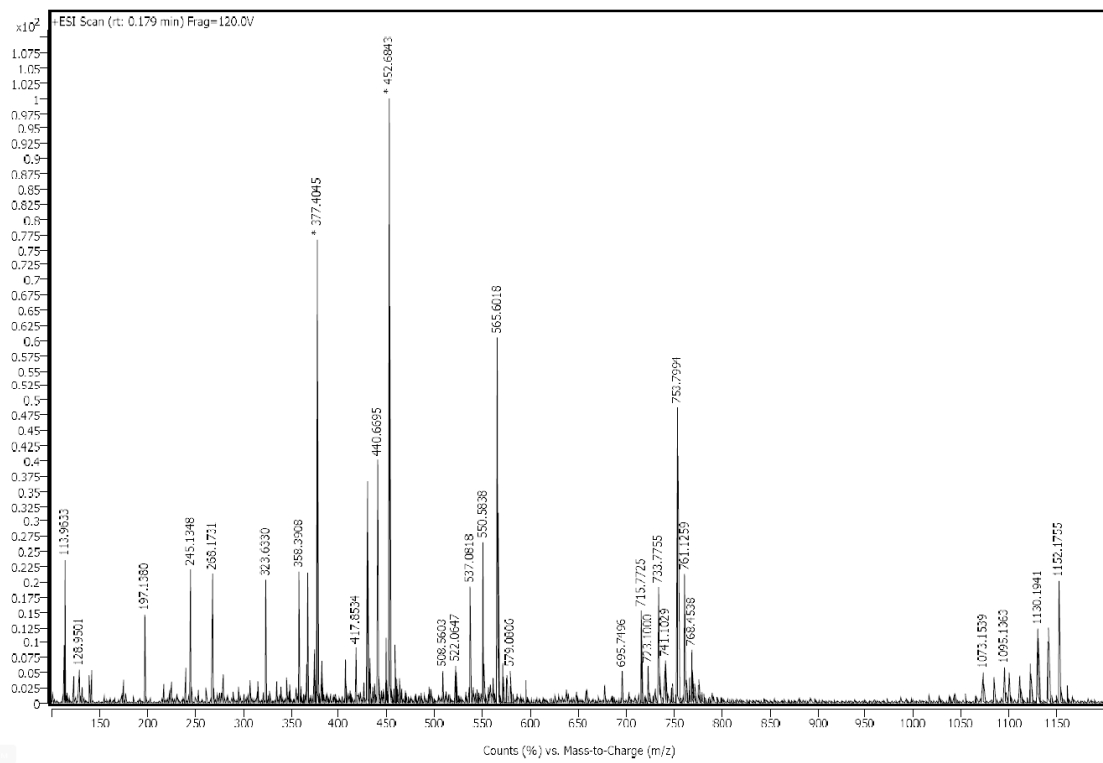


Fig. S19. Mass spectrum (HRESI) of G1-paco

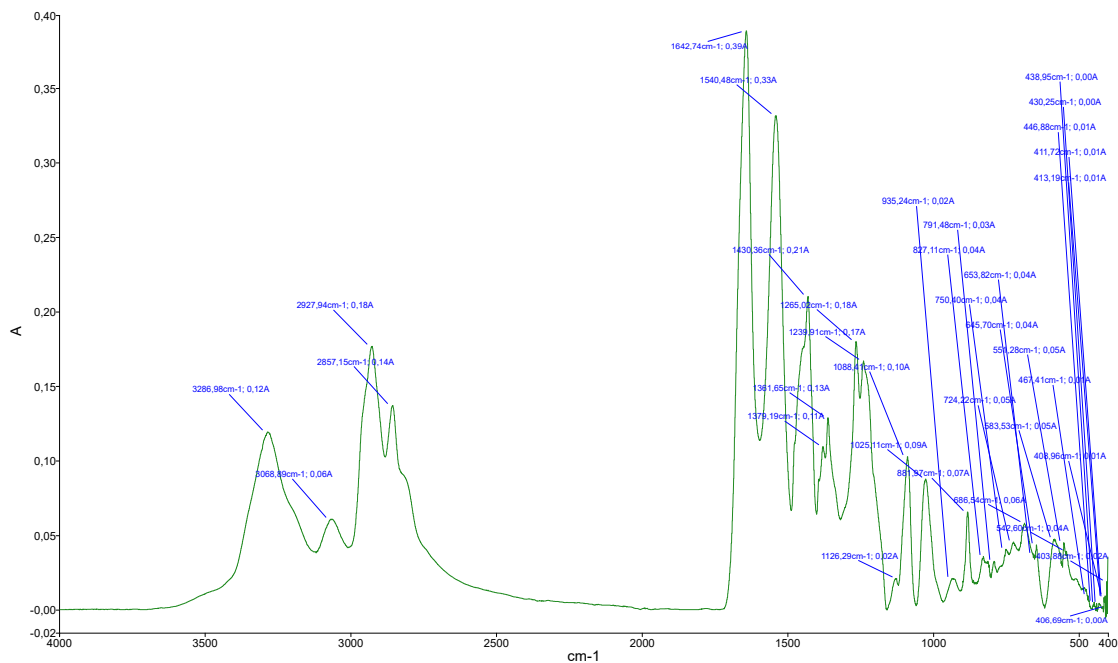


Fig. S20. FTIR-ATR spectrum of G1-paco

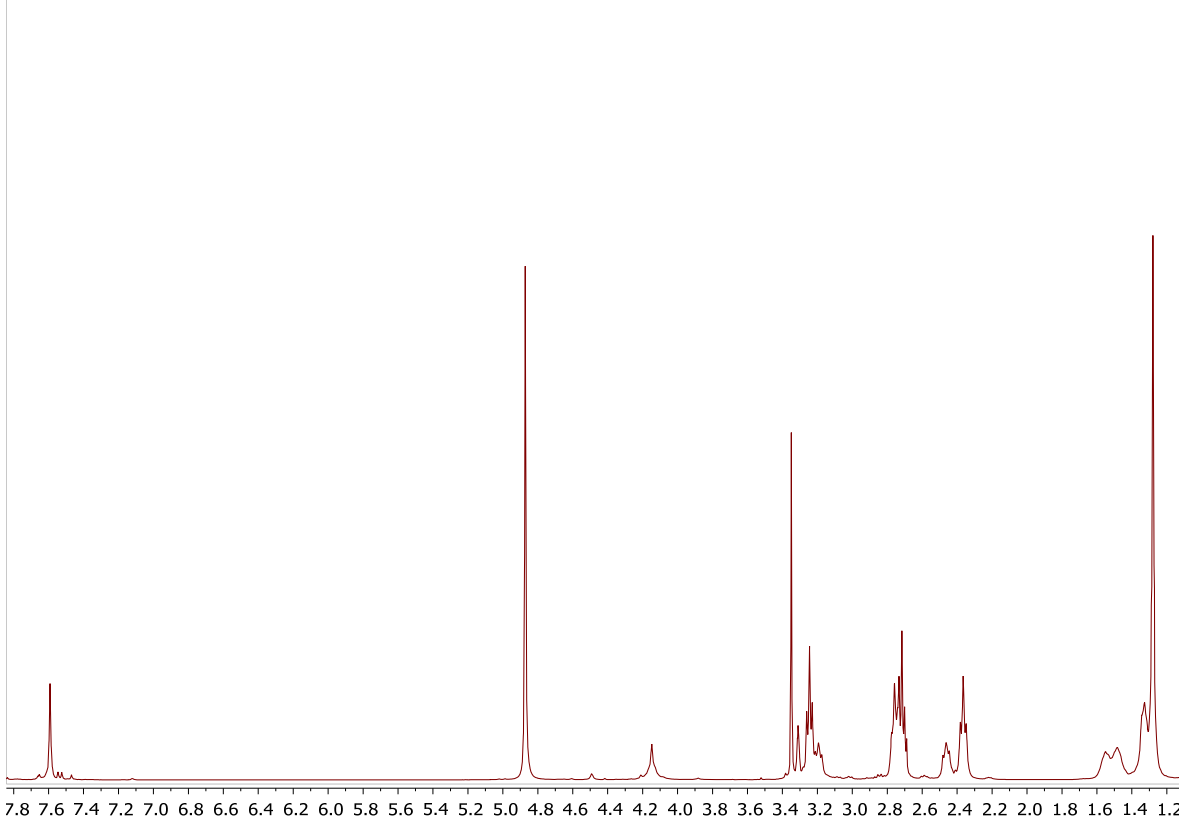


Fig. S21.  $^1\text{H}$  NMR spectrum of **G1-1,3-alt**,  $\text{CD}_3\text{OD}$ , 298 K, 400 MHz

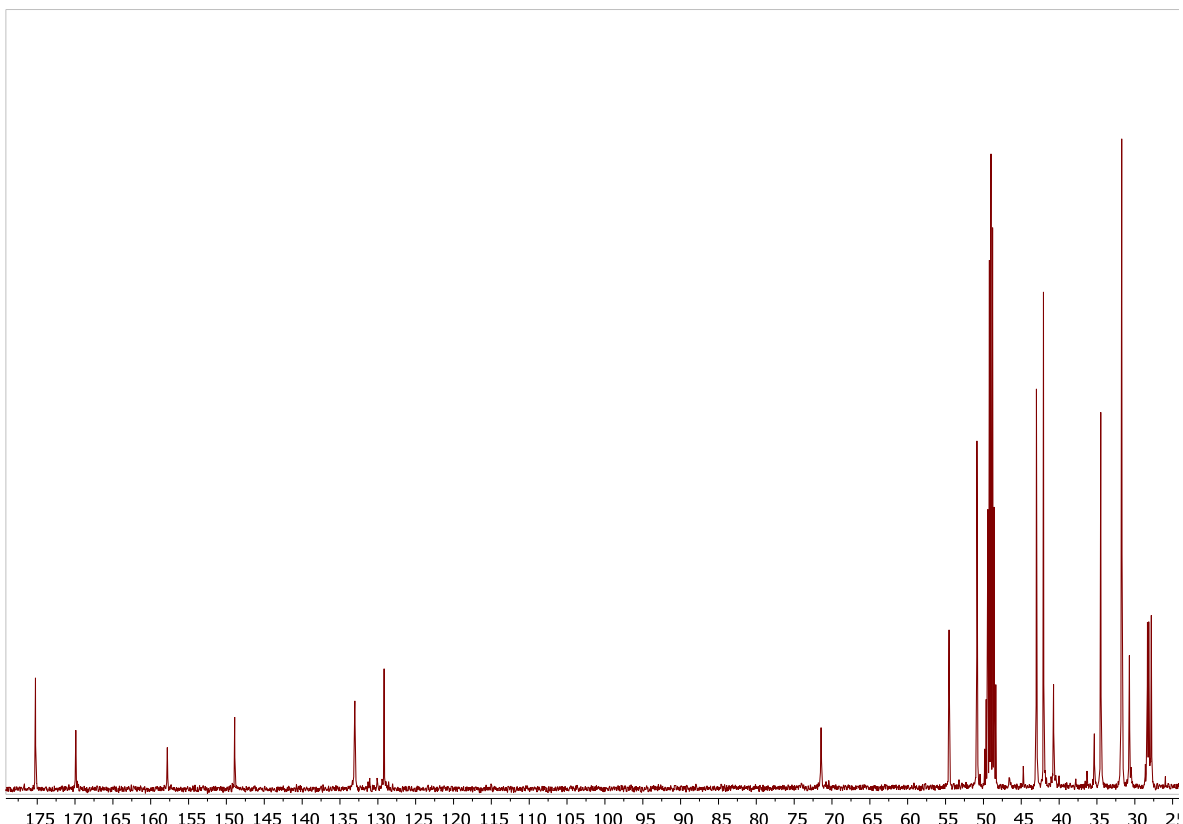


Fig. S22.  $^{13}\text{C}\{\text{H}\}$  NMR spectrum of **G1-1,3-alt**,  $\text{CD}_3\text{OD}$ , 298 K, 100 MHz

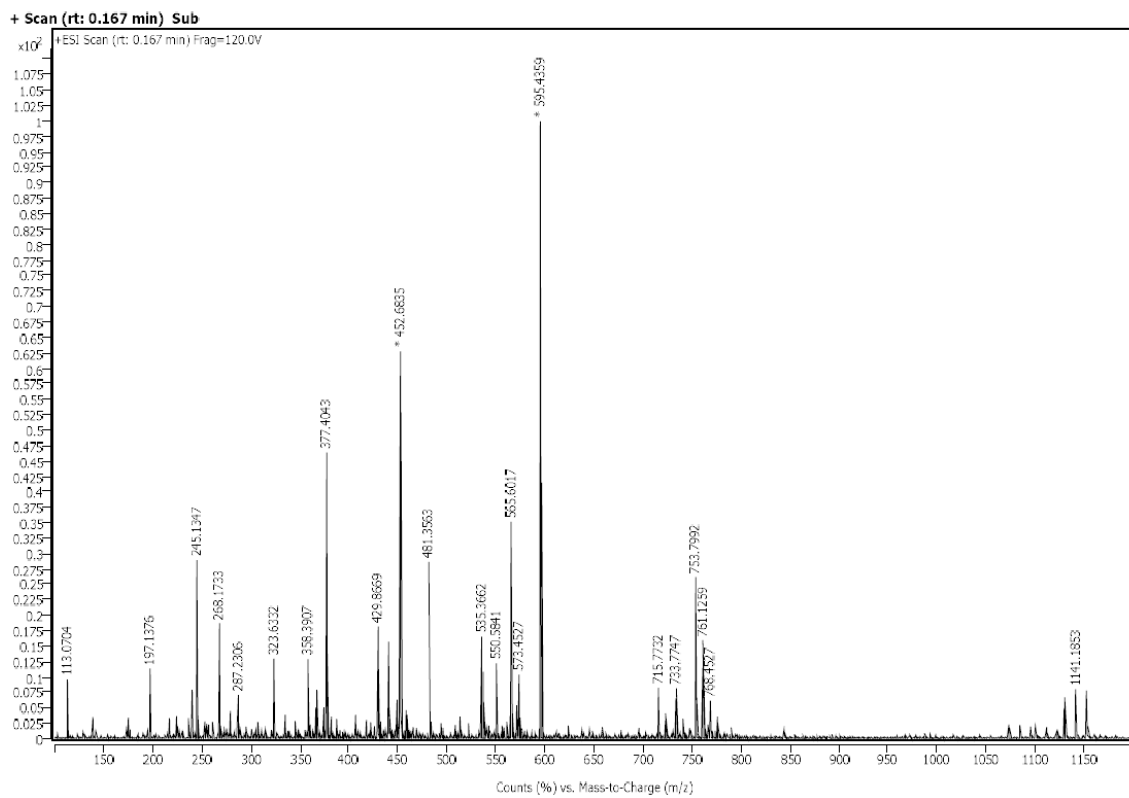


Fig. S23. Mass spectrum (HRESI) of G1-1,3-alt

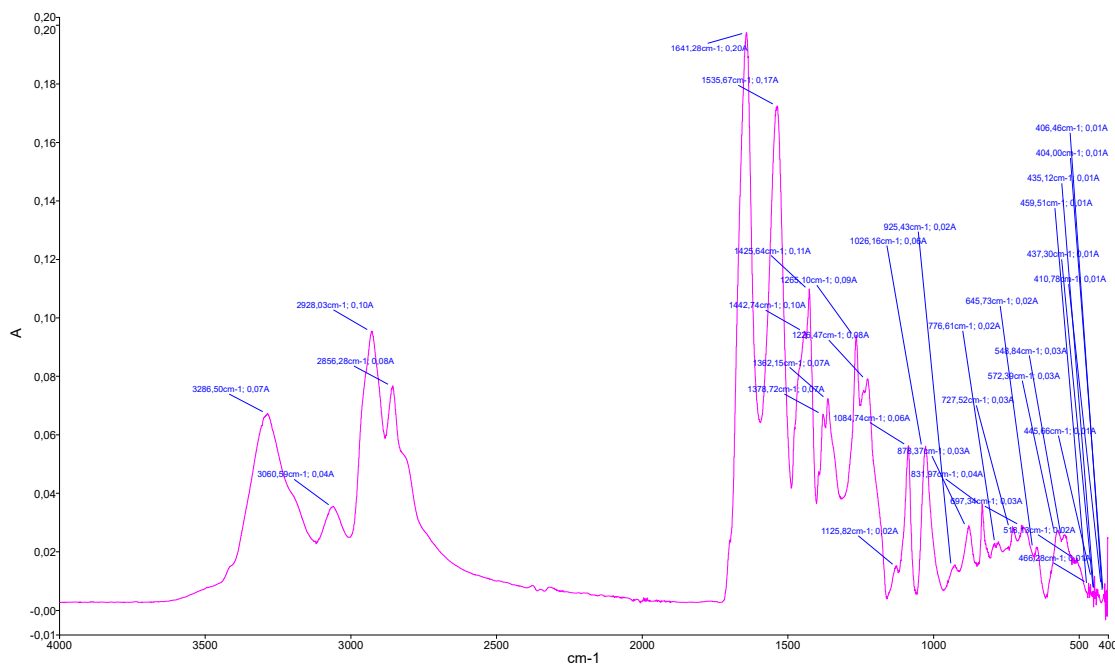


Fig. S24. FTIR-ATR spectrum of G1-1,3-alt

## 2. Complexation investigation

### 2.1. UV-Vis spectra

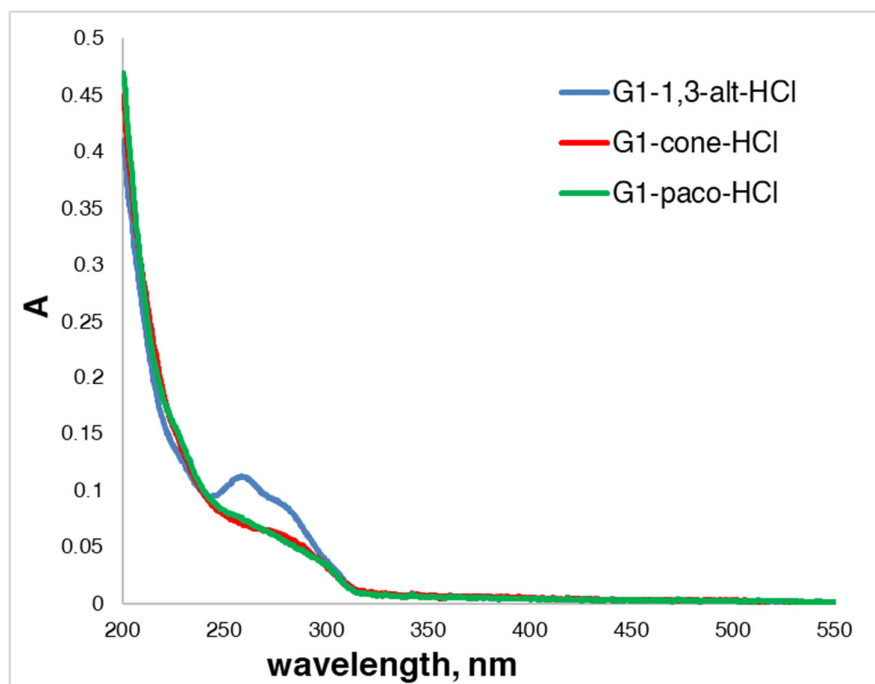


Fig. S25. UV-Vis absorption spectra of **G1-HCl** compounds ( $3.33 \mu\text{M}$ ) in different conformations, in 10 mM Tris-HCl, pH 7.4.

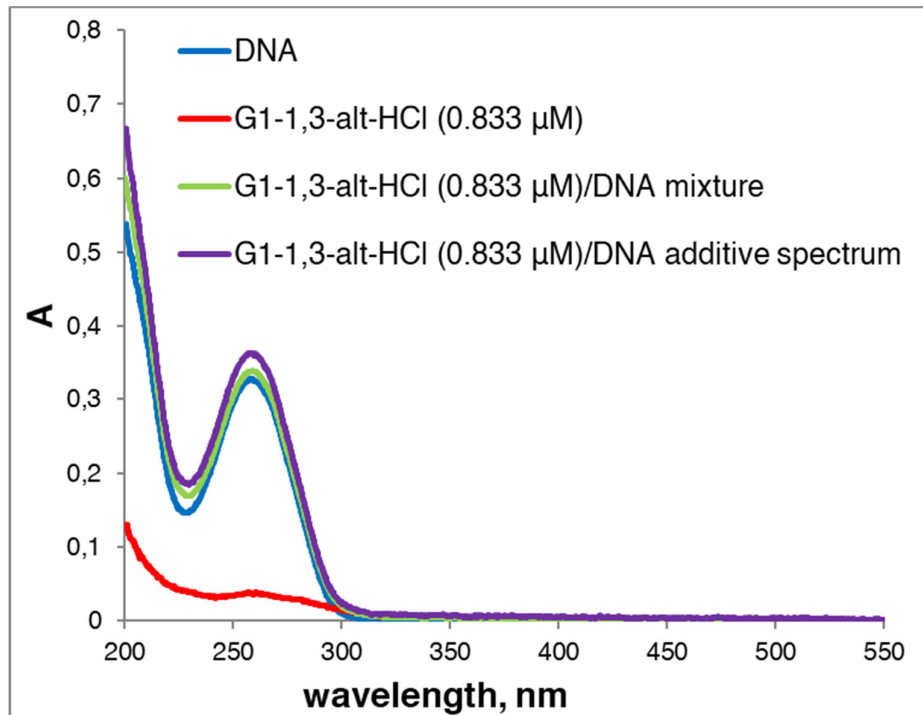


Fig. S26. UV-Vis absorption spectra of DNA ( $1.855 \times 10^{-5} \text{ M}$  base pairs), **G1-1,3-alt-HCl** ( $0.833 \mu\text{M}$ ), and their mixture in 10 mM Tris-HCl, pH 7.4.

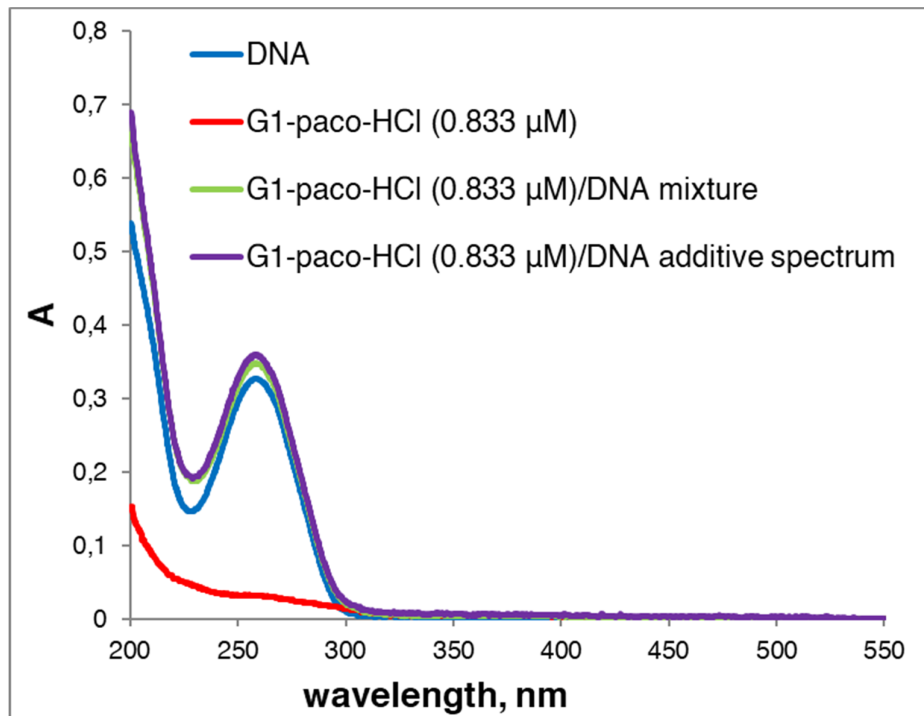


Fig. S27. UV-Vis absorption spectra of DNA ( $1.855 \times 10^{-5}$  M base pairs), **G1-paco-HCl** (0.833  $\mu$ M), and their mixture in 10 mM Tris-HCl, pH 7.4.

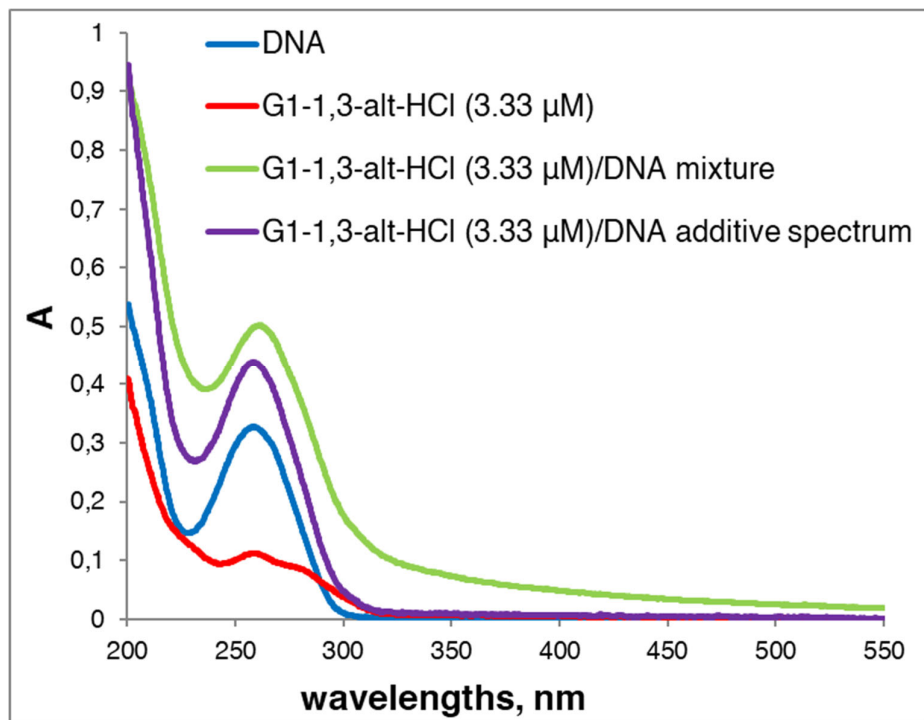


Fig. S28. UV-Vis absorption spectra of DNA ( $1.855 \times 10^{-5}$  M base pairs), **G1-1,3-alt-HCl** (3.33  $\mu$ M), and their mixture in 10 mM Tris-HCl, pH 7.4.

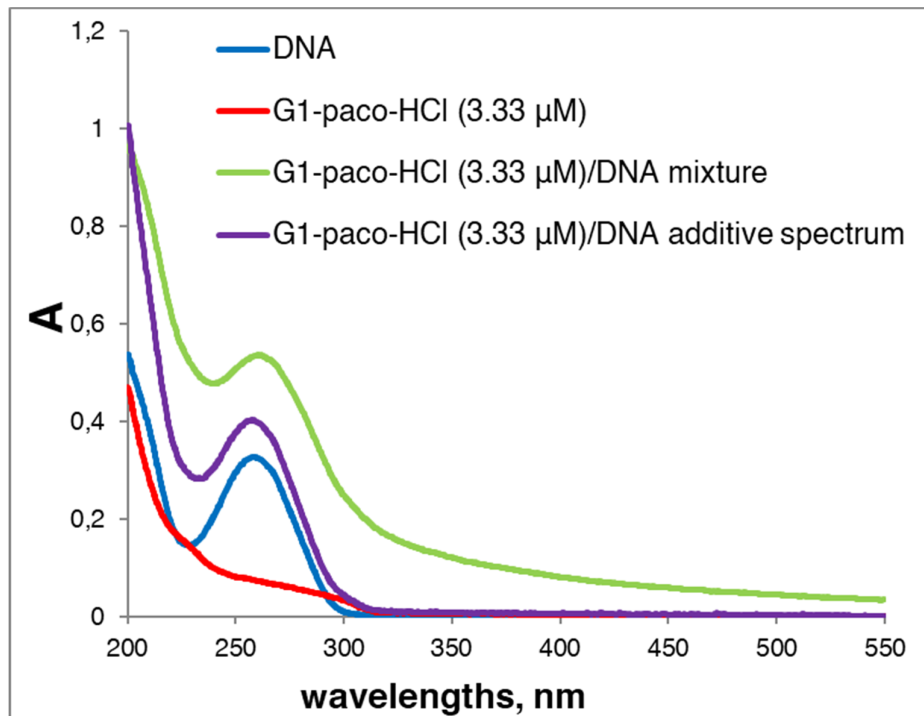


Fig. S29. UV-Vis absorption spectra of DNA ( $1.855 \times 10^{-5}$  M base pairs), **G1-paco-HCl** (3.33  $\mu\text{M}$ ), and their mixture in 10 mM Tris-HCl, pH 7.4.

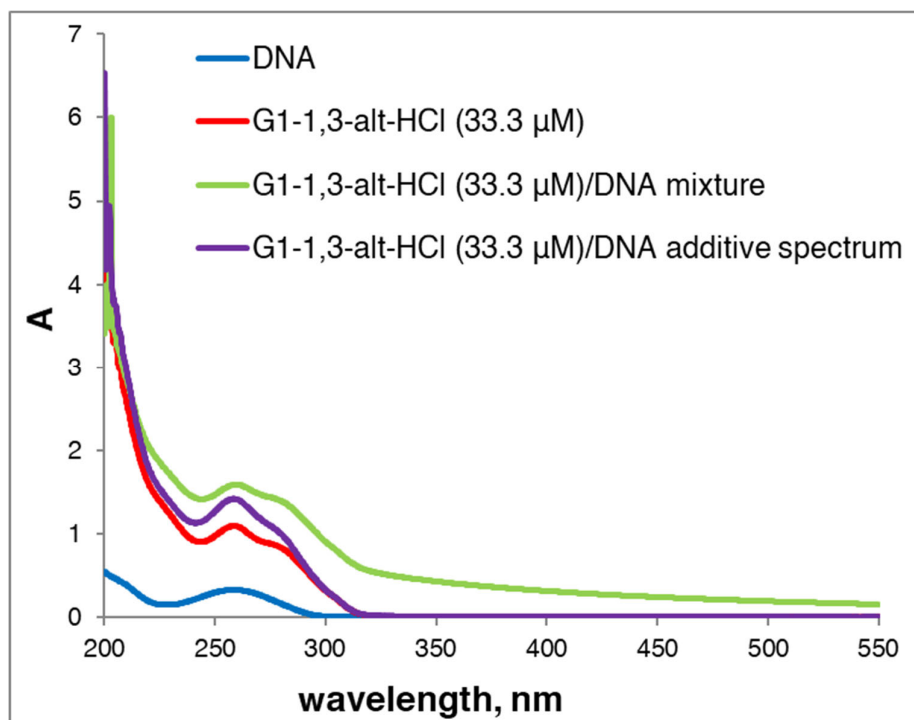


Fig. S30. UV-Vis absorption spectra of DNA ( $1.855 \times 10^{-5}$  M base pairs), **G1-1,3-alt-HCl** (33.3  $\mu\text{M}$ ), and their mixture in 10 mM Tris-HCl, pH 7.4.

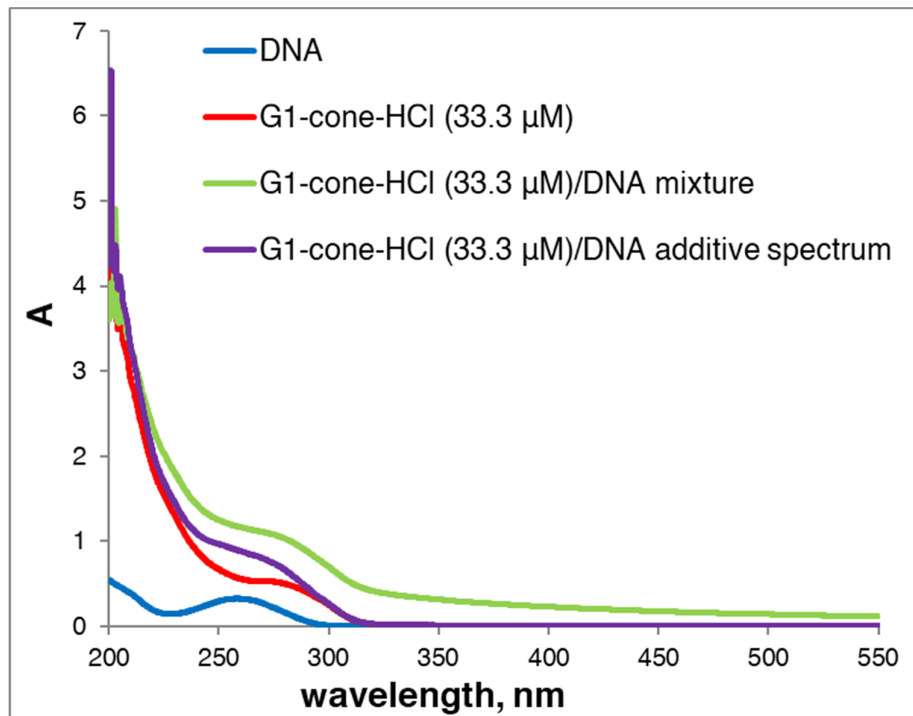


Fig. S31. UV-Vis absorption spectra of DNA ( $1.855 \times 10^{-5}$  M base pairs), **G1-cone-HCl** (33.3  $\mu$ M), and their mixture in 10 mM Tris-HCl, pH 7.4.

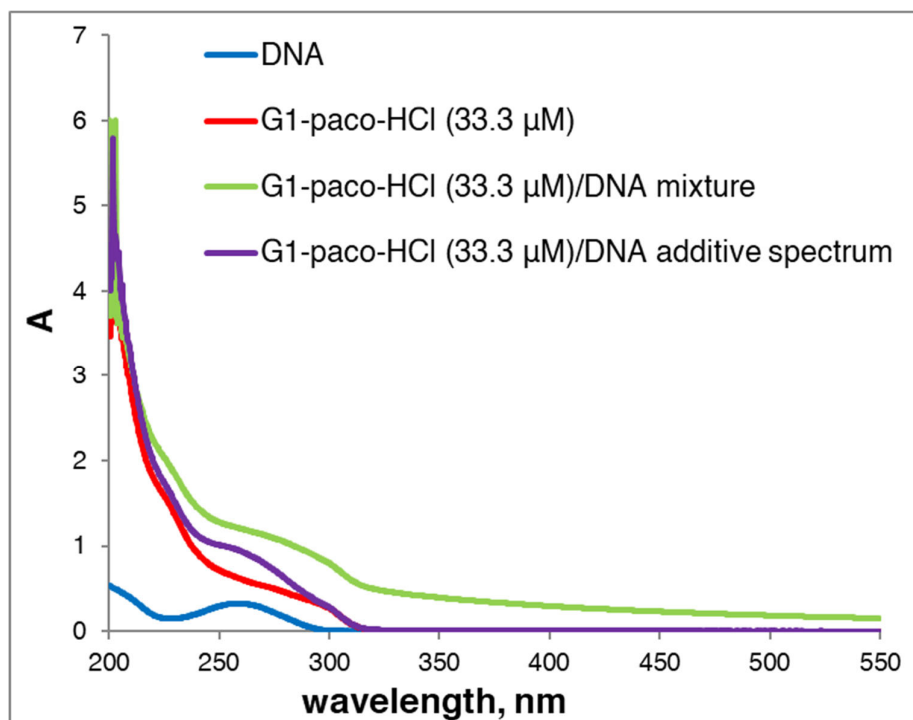


Fig. S32. UV-Vis absorption spectra of DNA ( $1.855 \times 10^{-5}$  M base pairs), **G1-paco-HCl** (33.3  $\mu$ M), and their mixture in 10 mM Tris-HCl, pH 7.4.

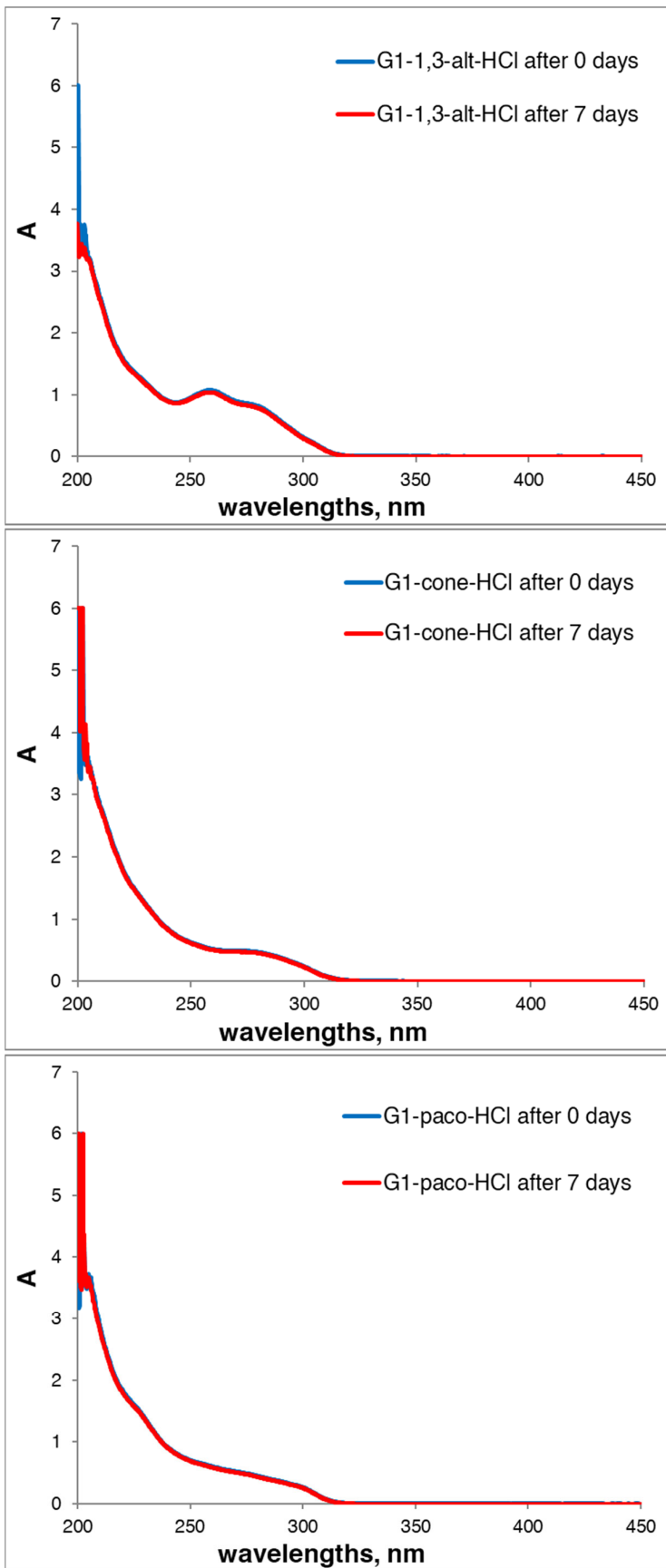


Fig. S33. UV-Vis spectra of compounds **G1-HCl** (33.3  $\mu$ M) in different conformations in 10 mM Tris-HCl (pH 7.4) immediately and after 7 days' storage at room temperature.

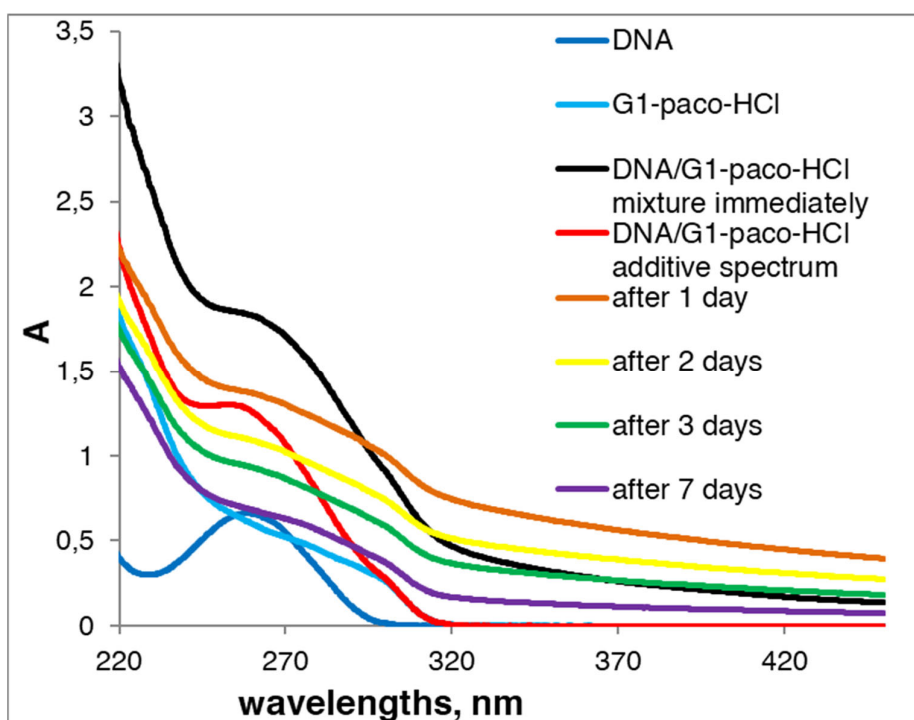
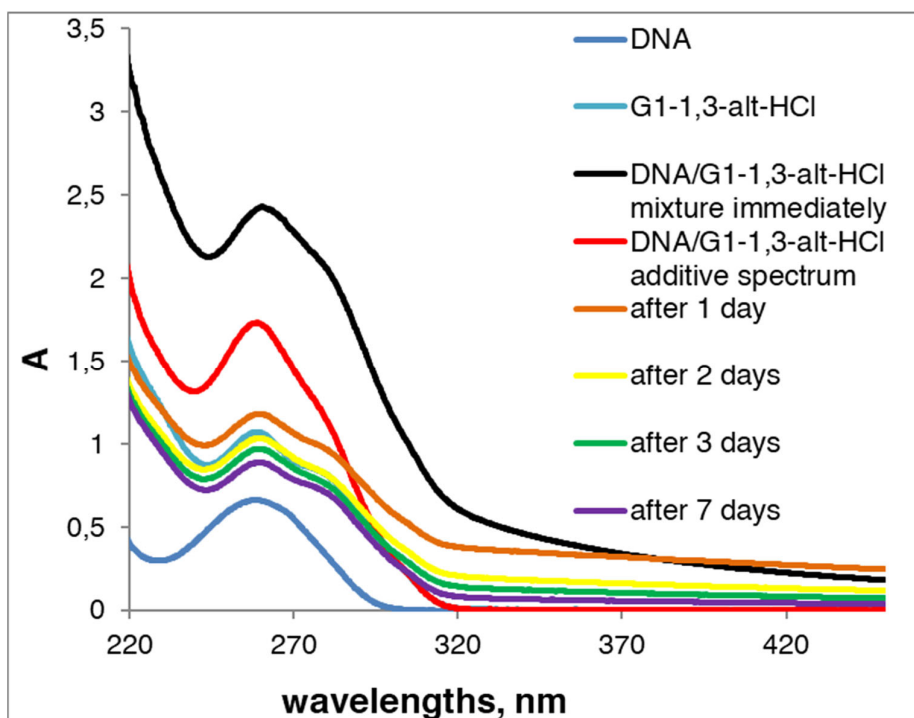


Fig. S34. UV-Vis spectra of compounds **G1-paco-HCl** and **G1-1,3-alt-HCl** (33.3  $\mu$ M), DNA ( $3.710 \times 10^{-5}$  M base pairs) and their mixture (10 mM Tris-HCl, pH 7.4) after storage at room temperature.

## 2.2 Fluorescence spectra

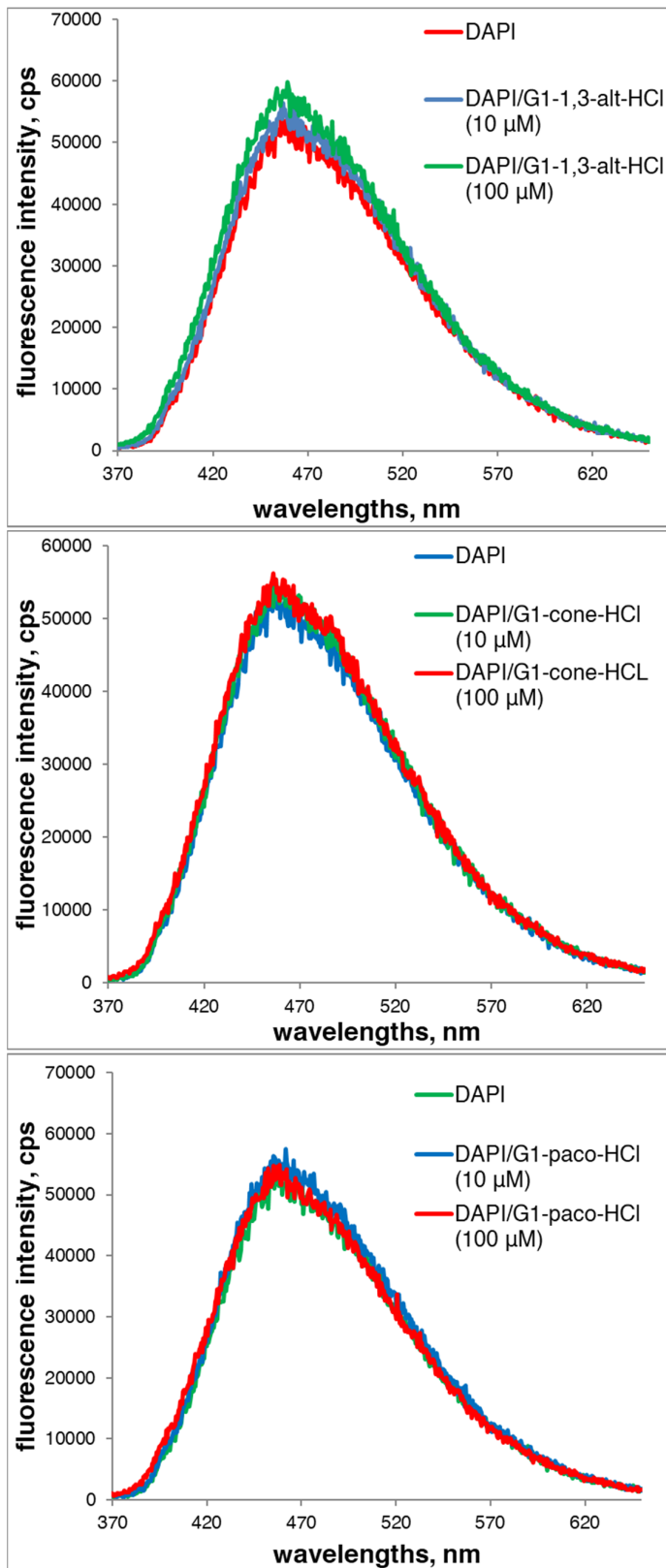


Fig. S35. Emission spectra of DAPI (10  $\mu\text{M}$ ) in presence of different conformations **G1-HCl** (10 and 100  $\mu\text{M}$ ) in 10 mM Tris-HCl, pH 7.4.

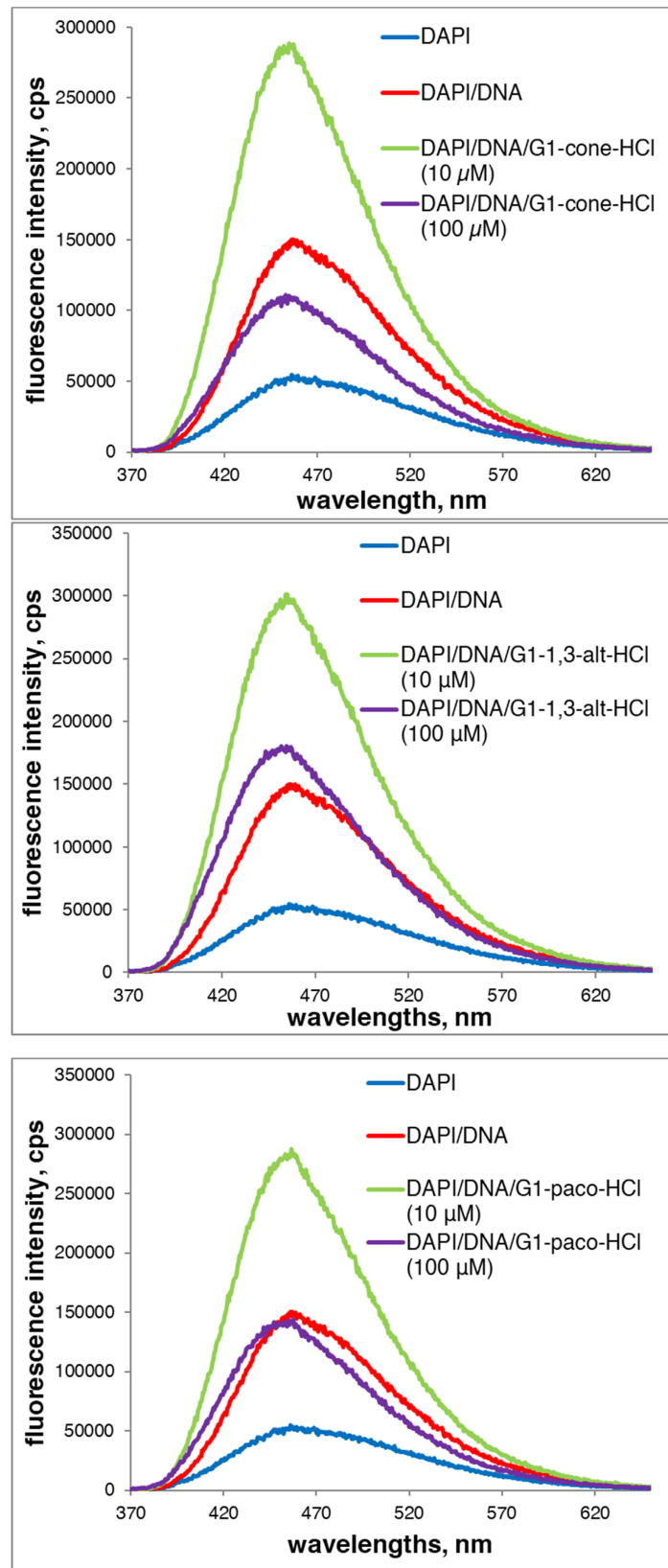


Fig. S36. Emission spectra of DAPI/DNA in presence of 10 and 100  $\mu\text{M}$  **G1-HCl**: DAPI added to DNA/dendrimer mixture.

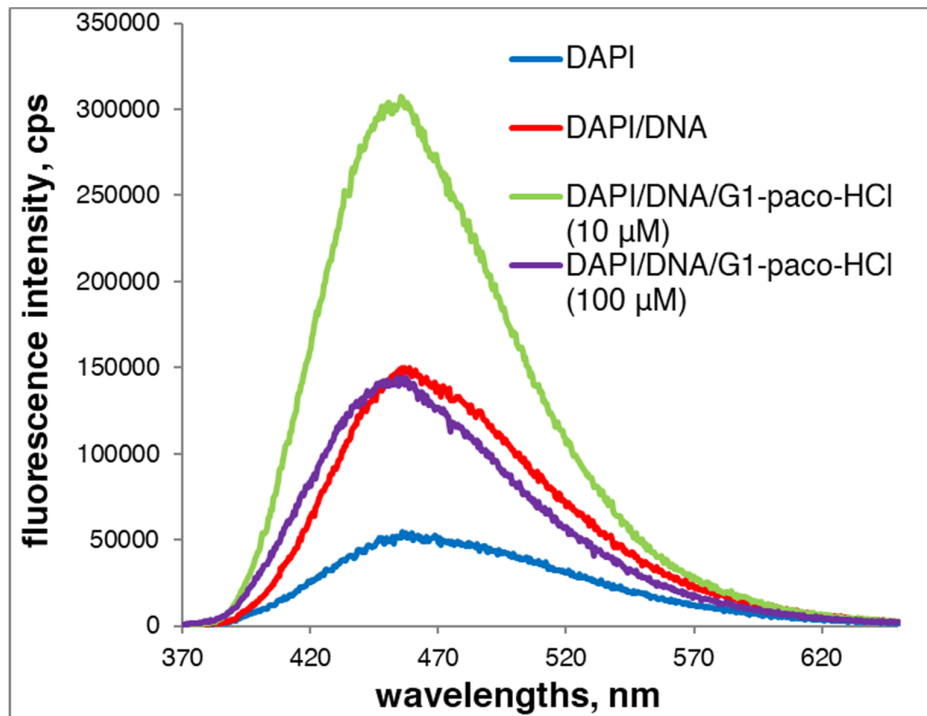


Fig. S37. Emission spectra of DAPI, DAPI/DNA and DAPI/DNA in the presence of 10  $\mu$ M and 100  $\mu$ M of **G1-paco-HCl**, in 10 mM Tris-HCl buffer, pH = 7.4: dendrimers added to DNA/DAPI mixture.

### 2.3. CD spectra

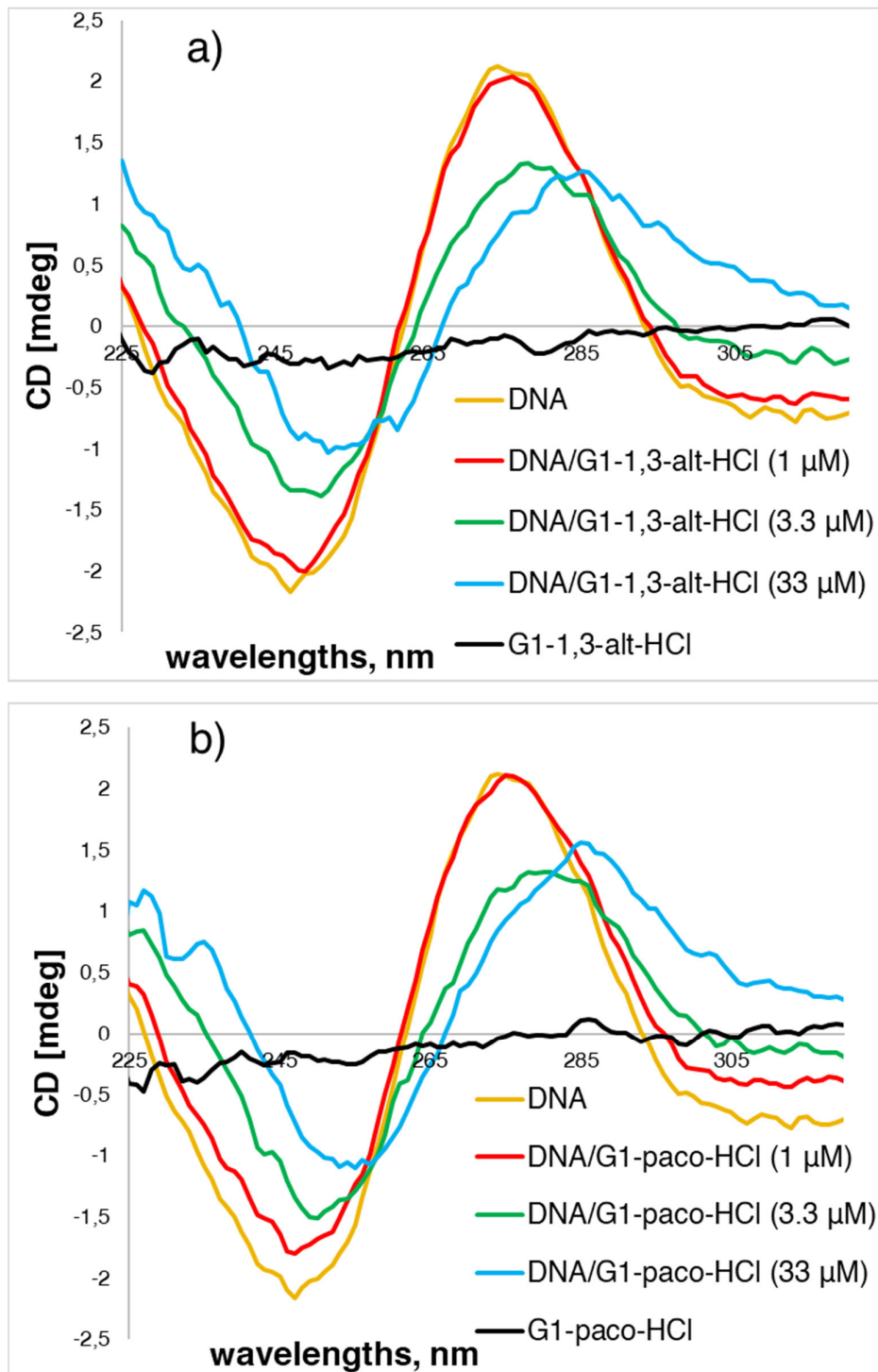


Fig. S38. CD spectra of salmon sperm DNA alone and in the presence of different concentrations of a) **G1-1,3-alt-HCl** and b) **G1-paco-HCl** in 10 mM Tris-HCl, pH 7.4.

#### 2.4. DLS data

**Table S1.** Size distributions (by intensity) of G1-HCl aggregates (10 mM Tris-HCl, pH 7.4).

Compound	C (G1-HCl), $\mu\text{M}$	$d_1, \text{nm}(\%)$	$d_2, \text{nm}(\%)$	$d_3, \text{nm}(\%)$	PDI
G1-1,3-alt-HCl	500	178.9 $\pm$ 46.2 (71.3 $\pm$ 16.7)	359.7 $\pm$ 315.6 (22.5 $\pm$ 17.9)	843.1 $\pm$ 2056 (3.7 $\pm$ 3.1)	0.532 $\pm$ 0.087
	100	316.6 $\pm$ 127.3 (70.2 $\pm$ 19.3)	57.2 $\pm$ 59.1 (22.5 $\pm$ 17.6)	1823 $\pm$ 2818 (5.1 $\pm$ 2.0)	0.398 $\pm$ 0.053
	50	269.0 $\pm$ 72.8 (83.7 $\pm$ 7.9)	34.0 $\pm$ 35.0 (9.6 $\pm$ 4.9)	1799 $\pm$ 2765 (3.9 $\pm$ 2.2)	0.386 $\pm$ 0.096
	10	243.5 $\pm$ 52.5 (84.8 $\pm$ 9.7)	896.6 $\pm$ 2105.0 (10.8 $\pm$ 8.5)	3519 $\pm$ 2723 (4.5 $\pm$ 2.4)	0.362 $\pm$ 0.048
	5	260.8 $\pm$ 40.0 (71.3 $\pm$ 16.7)	4935 $\pm$ 82.6 (8.6 $\pm$ 1.1)	14.2 $\pm$ 21.9 (1.9 $\pm$ 3.0)	0.312 $\pm$ 0.025
G1-cone-HCl	500	6.9 $\pm$ 1.9 (45.8 $\pm$ 9.4)	119.1 $\pm$ 125.1 (26.7 $\pm$ 4.2)	149.3 $\pm$ 189.2 (18.1 $\pm$ 7.2)	0.345 $\pm$ 0.104
	100	78.7 $\pm$ 176.2 (47.5 $\pm$ 6.0)	288.7 $\pm$ 159.0 (39.4 $\pm$ 5.1)	1802 $\pm$ 2708 (9.7 $\pm$ 4.1)	0.412 $\pm$ 0.199
	50	406.2 $\pm$ 136.4 (56.8 $\pm$ 7.4)	7.6 $\pm$ 2.0 (31.1 $\pm$ 9.6)	3376 $\pm$ 2612 (10.3 $\pm$ 2.6)	0.466 $\pm$ 0.188
	10	226.7 $\pm$ 23.0 (65.7 $\pm$ 9.0)	825.0 $\pm$ 1988 (18.9 $\pm$ 5.2)	3325 $\pm$ 2570 (12.8 $\pm$ 3.7)	0.352 $\pm$ 0.063
	5	206.3 $\pm$ 41.8 (65.5 $\pm$ 8.1)	849.0 $\pm$ 2035 (20.0 $\pm$ 4.6)	2502 $\pm$ 2728 (12.4 $\pm$ 3.4)	0.347 $\pm$ 0.141
G1-paco-HCl	500	378.1 $\pm$ 36.6 (63.4 $\pm$ 6.2)	2.2 $\pm$ 0.6 (26.7 $\pm$ 7.8)	931.2 $\pm$ 2268 (9.0 $\pm$ 4.0)	0.554 $\pm$ 0.147
	100	439.1 $\pm$ 33.7 (64.2 $\pm$ 5.7)	3.3 $\pm$ 1.0 (19.1 $\pm$ 5.2)	27.1 $\pm$ 23.3 (10.8 $\pm$ 2.8)	0.626 $\pm$ 0.120
	50	337.6 $\pm$ 53.4(87 .8 $\pm$ 3.7)	2.9 $\pm$ 0.6 (11.9 $\pm$ 3.2)	926.7 $\pm$ 2270 (0.3 $\pm$ 0.7)	0.539 $\pm$ 0.064
	10	337.8 $\pm$ 61.0 (82.8 $\pm$ 6.9)	30.4 $\pm$ 4.5 (14.7 $\pm$ 4.3)	2.6 $\pm$ 5.6 (2.5 $\pm$ 5.2)	0.699 $\pm$ 0.113
	5	356.3 $\pm$ 101.6 (86.8 $\pm$ 1.9)	34.1 $\pm$ 2.9 (12.7 $\pm$ 2.3)	928.9 $\pm$ 2269 (0.6 $\pm$ 0.9)	0.550 $\pm$ 0.074

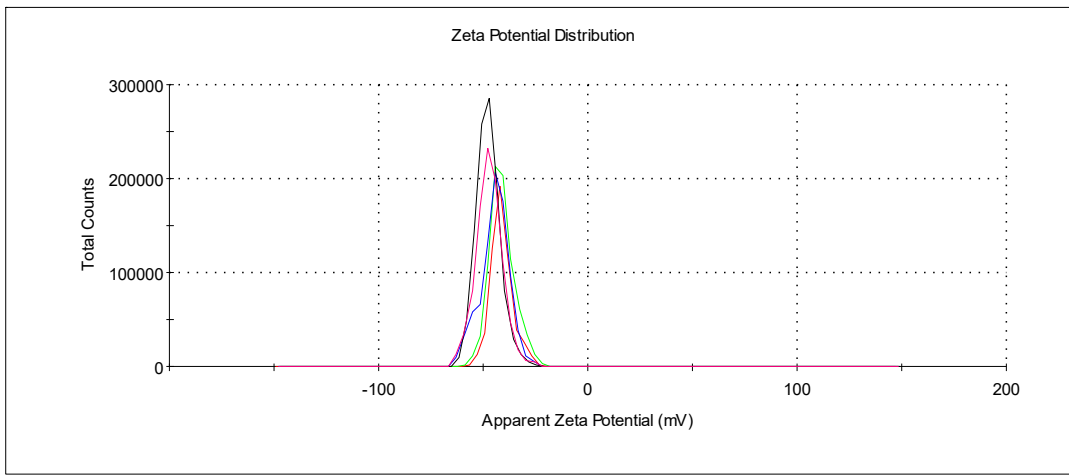


Fig. S39. Zeta-potential distributions of **G1-1,3-alt-HCl** ( $5 \mu\text{M}$ ) + DNA ( $5.565 \times 10^{-5} \text{ M}$  base pairs) aggregates.

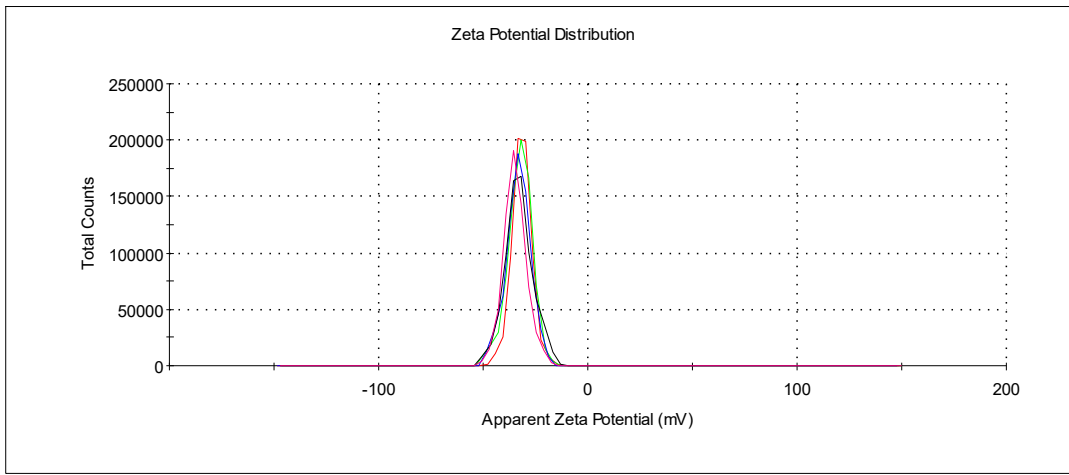


Fig. S40. Zeta-potential distributions of **G1-1,3-alt-HCl** ( $10 \mu\text{M}$ ) + DNA ( $5.565 \times 10^{-5} \text{ M}$  base pairs) aggregates.

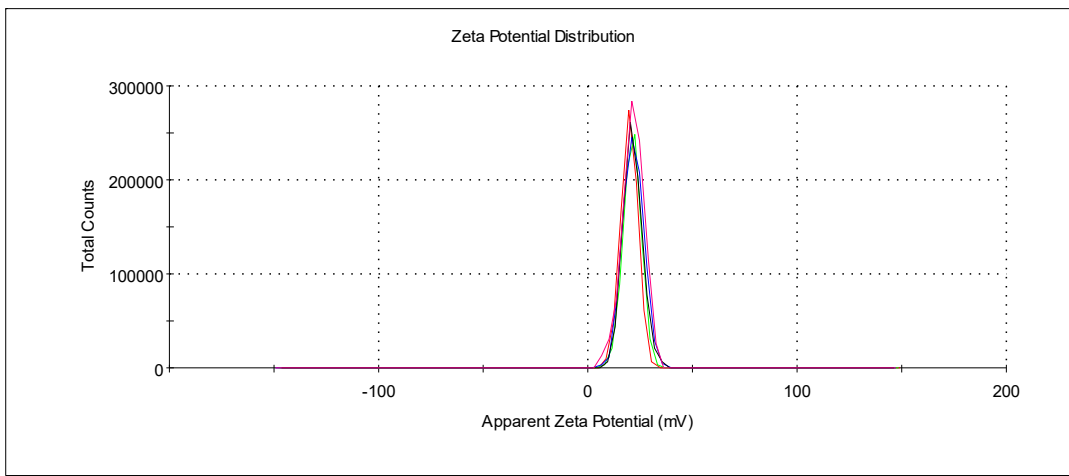


Fig. S41. Zeta-potential distributions of **G1-1,3-alt-HCl** ( $50 \mu\text{M}$ ) + DNA ( $5.565 \times 10^{-5} \text{ M}$  base pairs) aggregates.

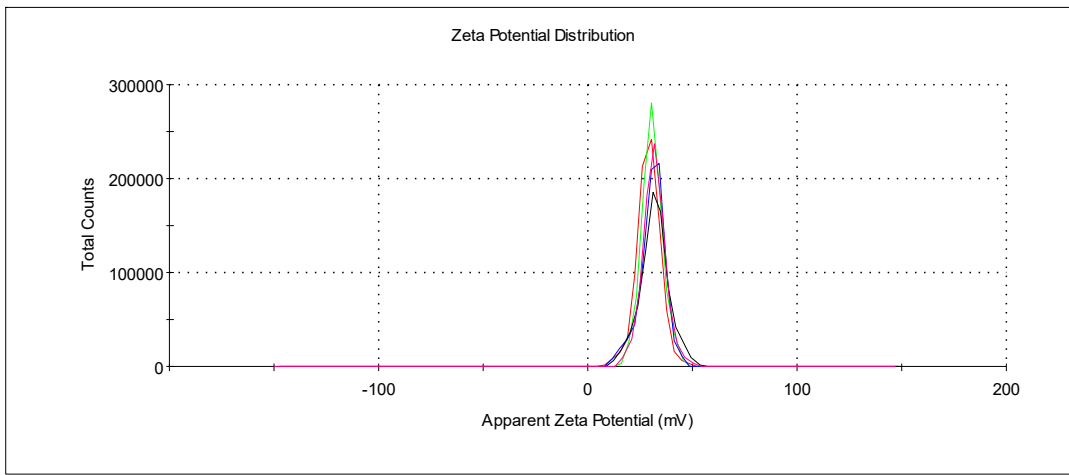


Fig. S42. Zeta-potential distributions of **G1-1,3-alt-HCl** (100  $\mu$ M) + DNA (5.565 $\times$ 10 $^{-5}$  M base pairs) aggregates.

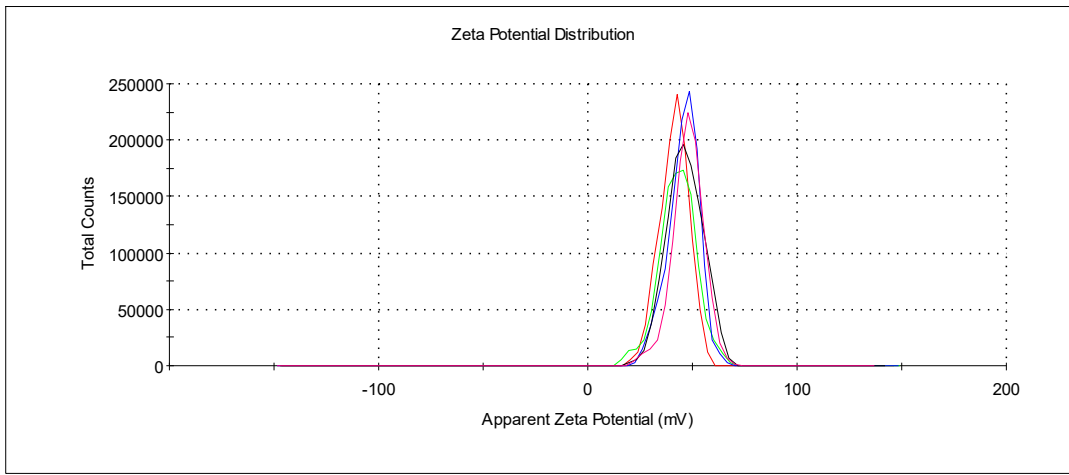


Fig. S43. Zeta-potential distributions of **G1-1,3-alt-HCl** (500  $\mu$ M) + DNA (5.565 $\times$ 10 $^{-5}$  M base pairs) aggregates.

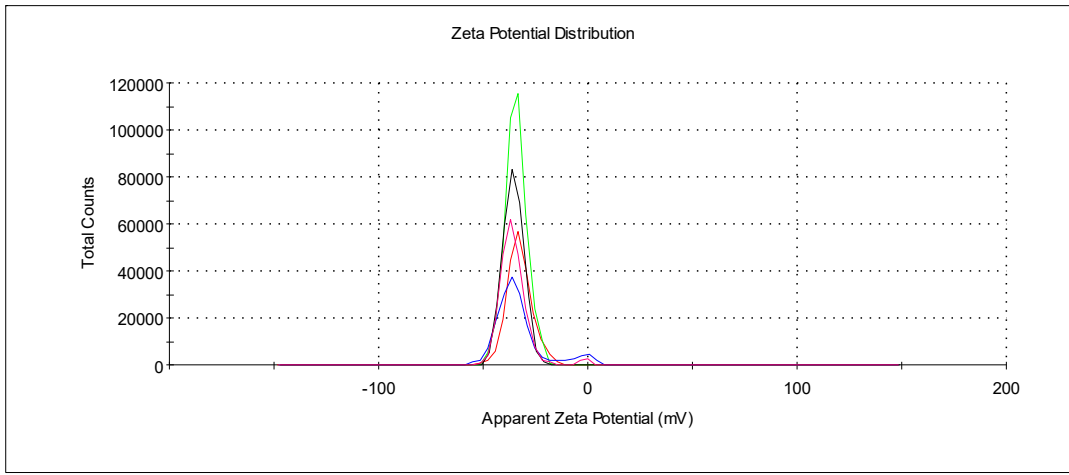


Fig. S44. Zeta-potential distributions of **G1-paco-HCl** (5  $\mu$ M) + DNA (5.565 $\times$ 10 $^{-5}$  M base pairs) aggregates.

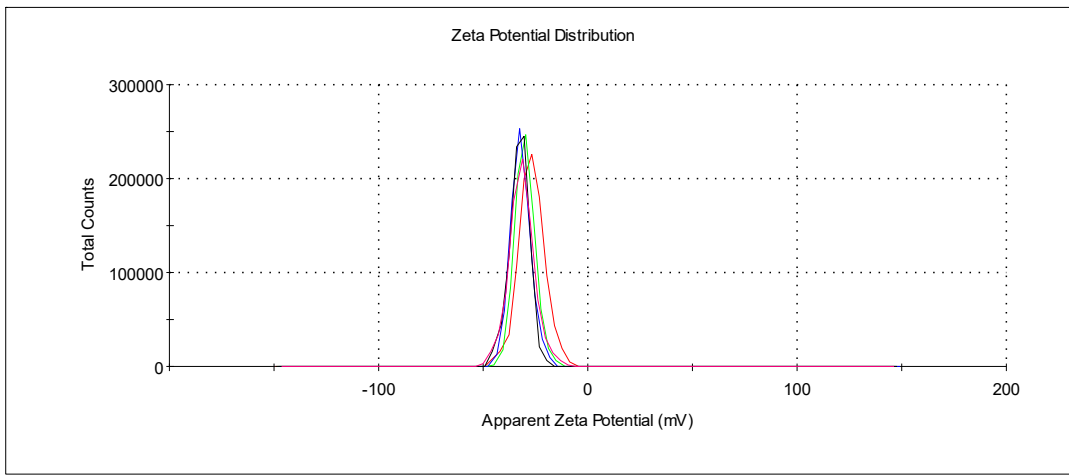


Fig. S45. Zeta-potential distributions of **G1-paco-HCl** (10  $\mu$ M) + DNA (5.565 $\times$ 10 $^{-5}$  M base pairs) aggregates.

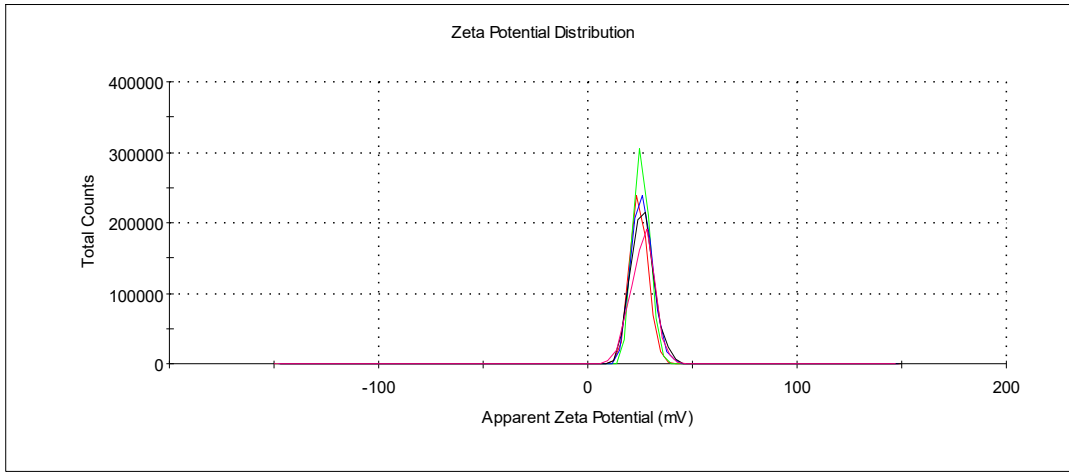


Fig. S46. Zeta-potential distributions of **G1-paco-HCl** (50  $\mu$ M) + DNA (5.565 $\times$ 10 $^{-5}$  M base pairs) aggregates.

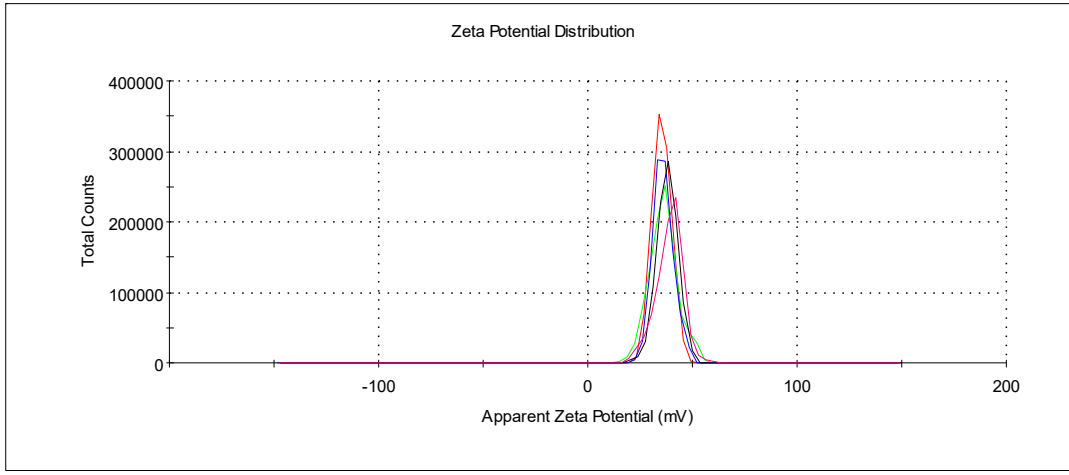


Fig. S47. Zeta-potential distributions of **G1-paco-HCl** (100  $\mu$ M) + DNA (5.565 $\times$ 10 $^{-5}$  M base pairs) aggregates.

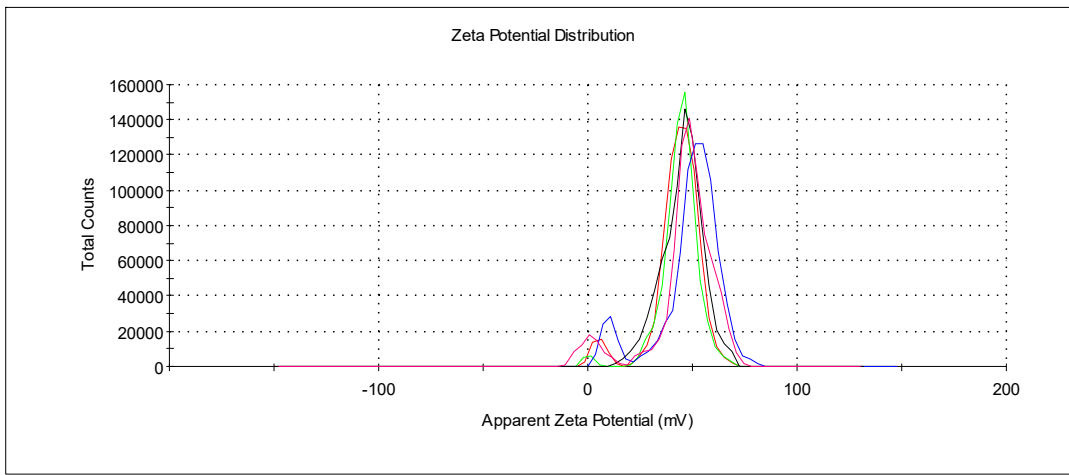


Fig. S48. Zeta-potential distributions of **G1-paco-HCl** ( $500 \mu\text{M}$ ) + DNA ( $5.565 \times 10^{-5} \text{ M}$  base pairs) aggregates.

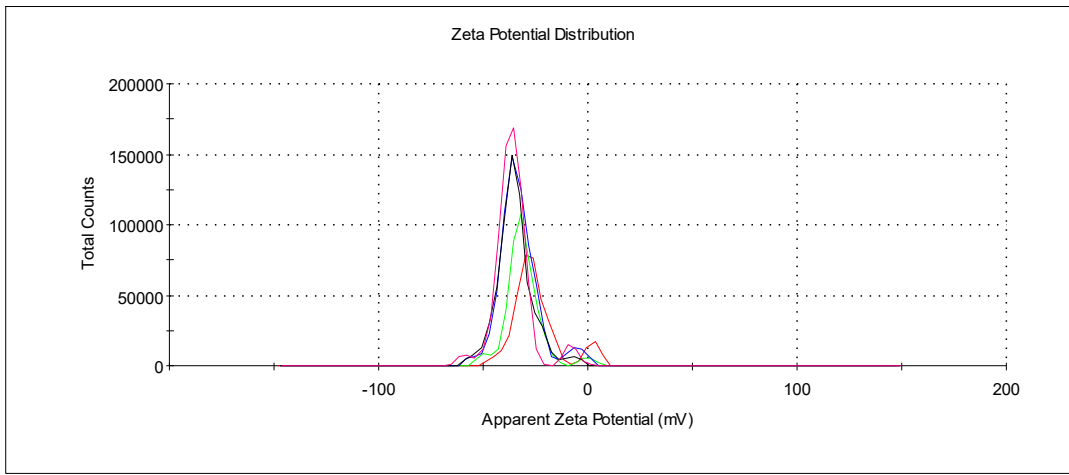


Fig. S49. Zeta-potential distributions of **G1-cone-HCl** ( $5 \mu\text{M}$ ) + DNA ( $5.565 \times 10^{-5} \text{ M}$  base pairs) aggregates.

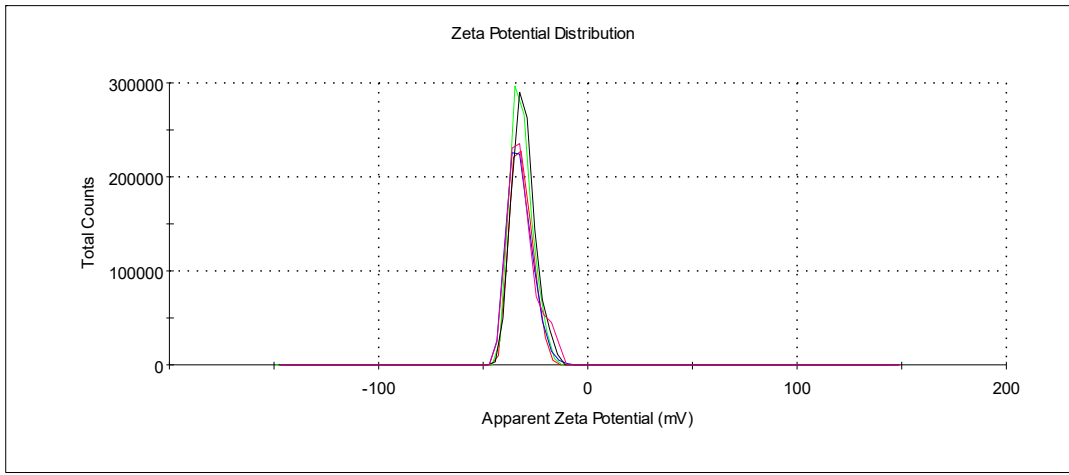


Fig. S50. Zeta-potential distributions of **G1-cone-HCl** ( $10 \mu\text{M}$ ) + DNA ( $5.565 \times 10^{-5} \text{ M}$  base pairs) aggregates.

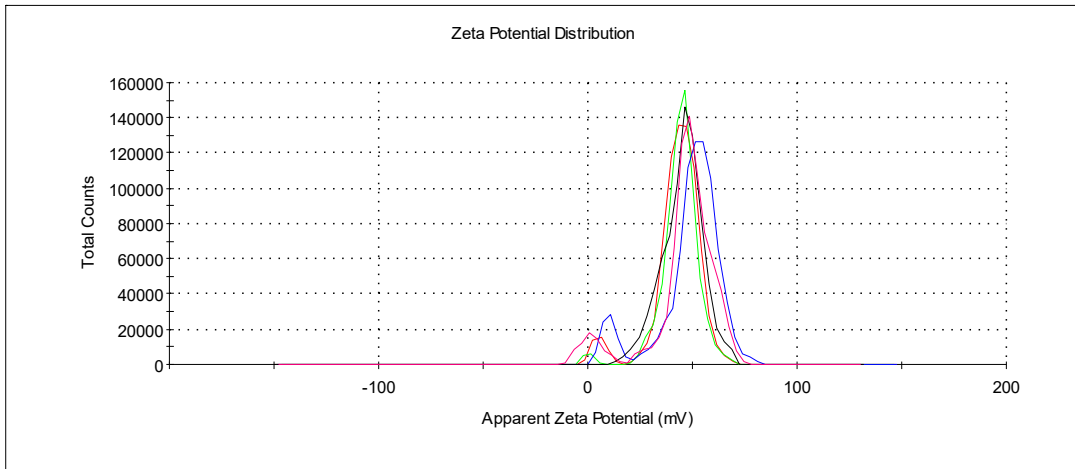


Fig. S51. Zeta-potential distributions of **G1-cone-HCl** (50  $\mu$ M) + DNA (5.565 $\times$ 10 $^{-5}$  M base pairs) aggregates.

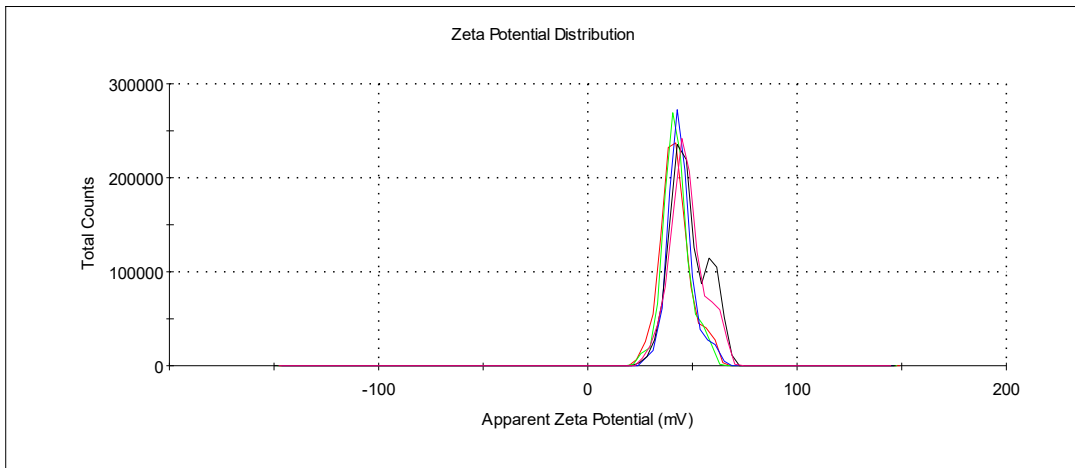


Fig. S52. Zeta-potential distributions of **G1-cone-HCl** (100  $\mu$ M) + DNA (5.565 $\times$ 10 $^{-5}$  M base pairs) aggregates.

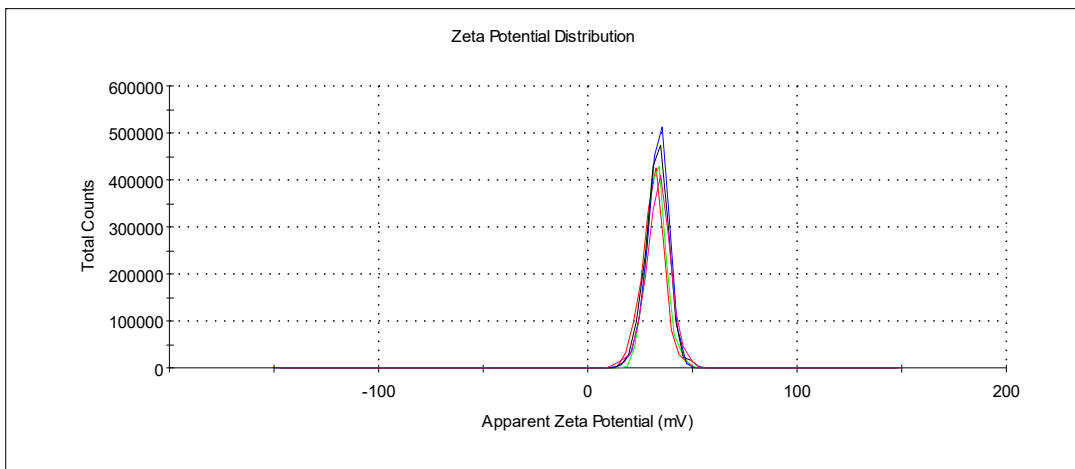


Fig. S53. Zeta-potential distributions of **G1-cone-HCl** (500  $\mu$ M) + DNA (5.565 $\times$ 10 $^{-5}$  M base pairs) aggregates.

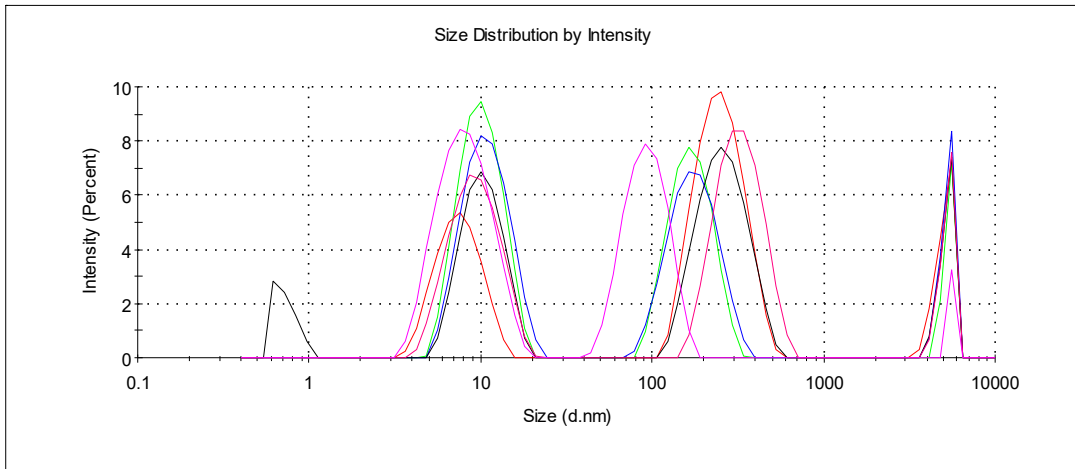


Fig. S54. Size distributions of DNA ( $5.565 \times 10^{-5}$  M base pairs).

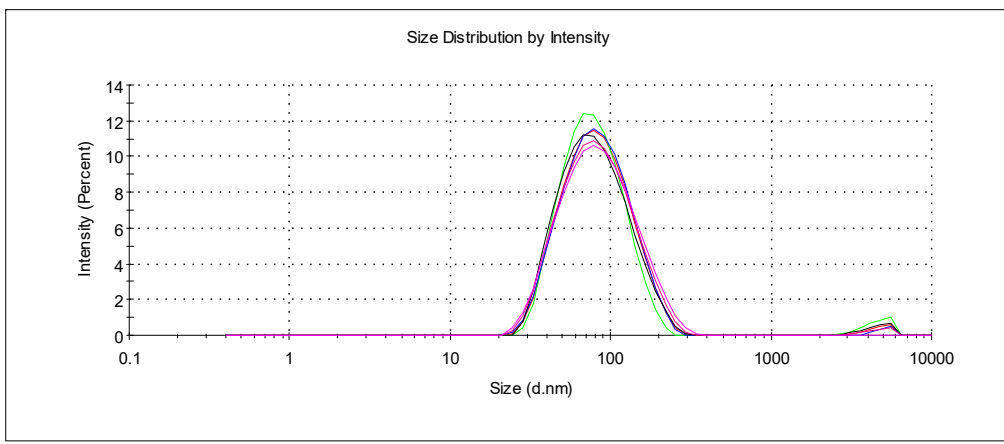


Fig. S55. Size distributions of **G1-1,3-alt-HCl** (500  $\mu$ M) + DNA ( $5.565 \times 10^{-5}$  M base pairs) aggregates.

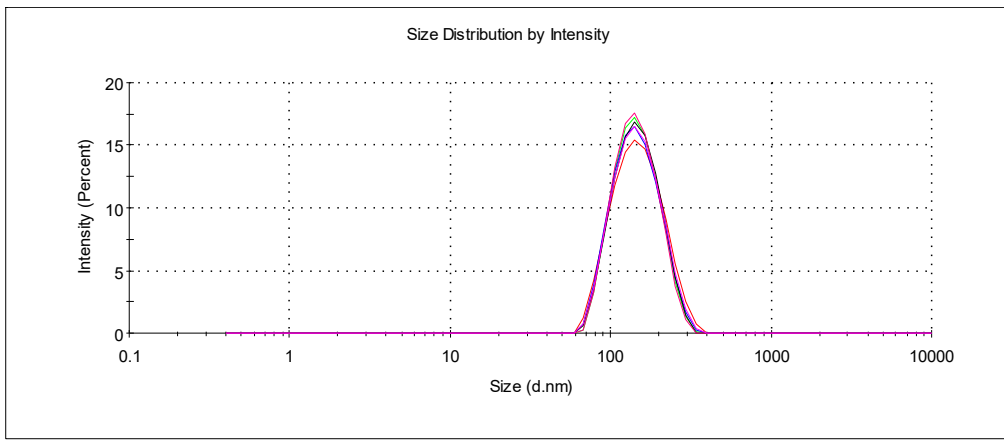


Fig. S56. Size distributions of **G1-1,3-alt-HCl** (100  $\mu$ M) + DNA ( $5.565 \times 10^{-5}$  M base pairs) aggregates.

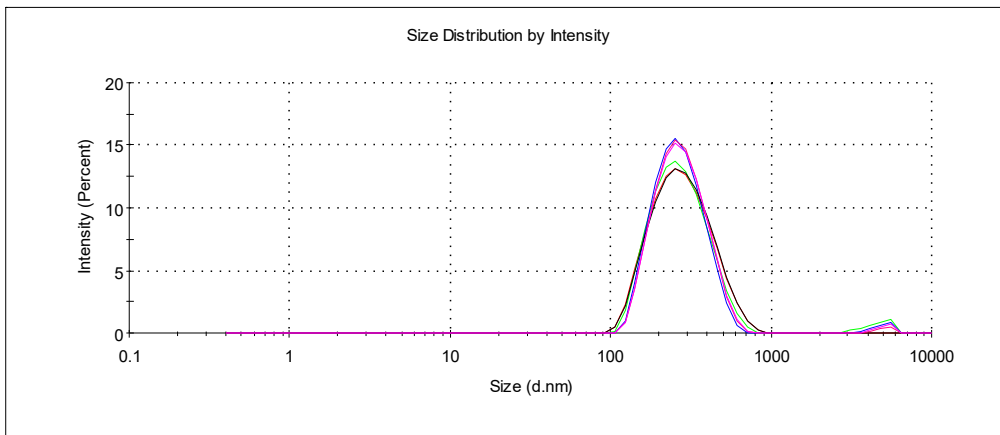


Fig. S57. Size distributions of **G1-1,3-alt-HCl** (50  $\mu\text{M}$ ) + DNA ( $5.565 \times 10^{-5}$  M base pairs) aggregates.

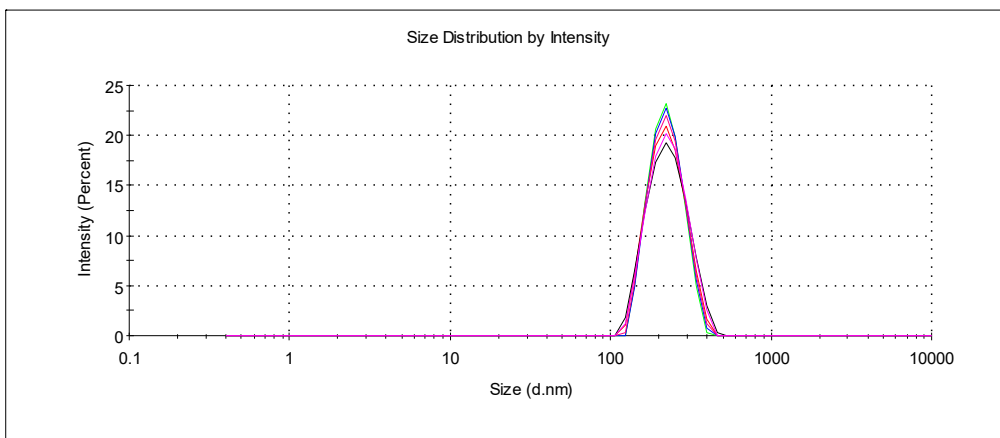


Fig. S58. Size distributions of **G1-1,3-alt-HCl** (10  $\mu\text{M}$ ) + DNA ( $5.565 \times 10^{-5}$  M base pairs) aggregates.

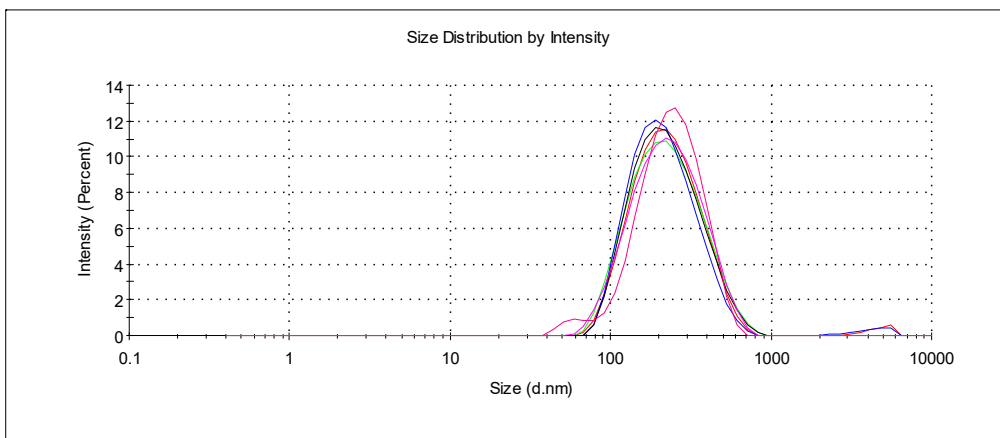


Fig. S59. Size distributions of **G1-1,3-alt-HCl** (5  $\mu\text{M}$ ) + DNA ( $5.565 \times 10^{-5}$  M base pairs) aggregates.

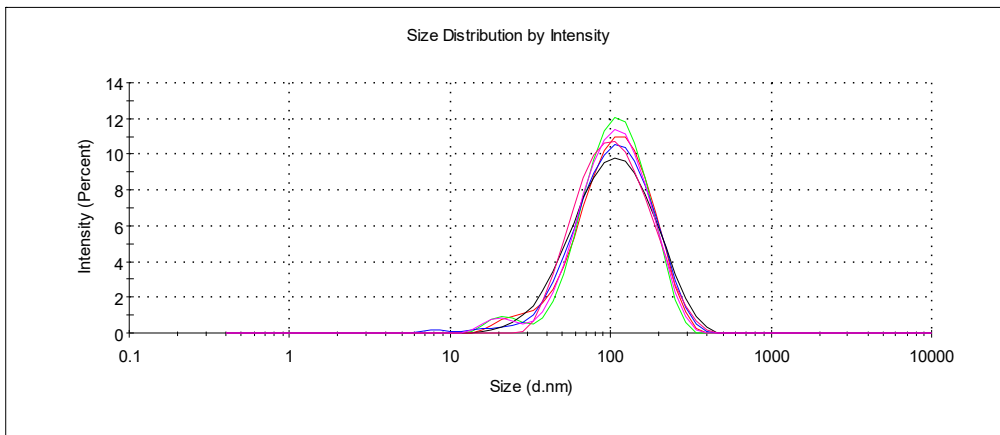


Fig. S60. Size distributions of **G1-cone-HCl** (500  $\mu\text{M}$ ) + DNA ( $5.565 \times 10^{-5}$  M base pairs) aggregates.

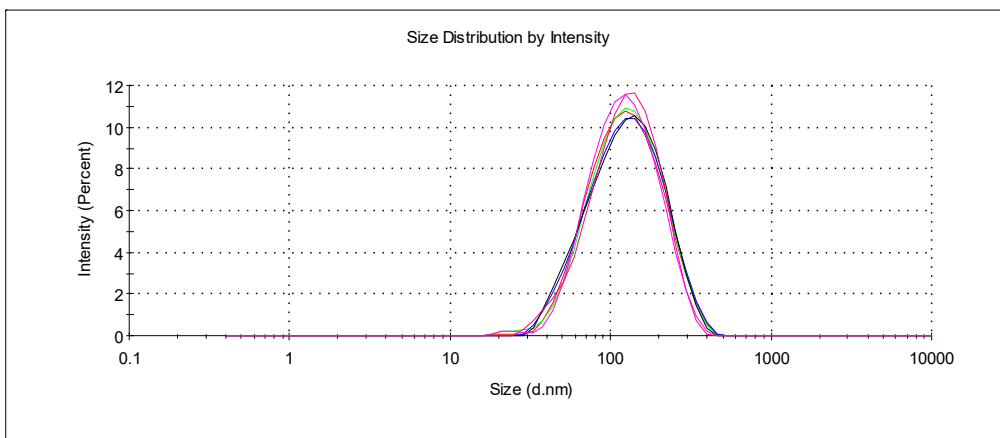


Fig. S61. Size distributions of **G1-cone-HCl** (100  $\mu\text{M}$ ) + DNA ( $5.565 \times 10^{-5}$  M base pairs) aggregates.

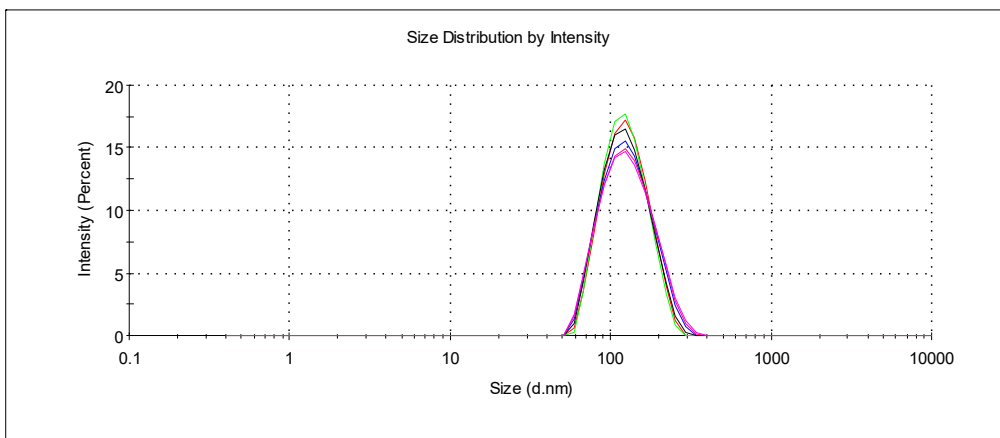


Fig. S62. Size distributions of **G1-cone-HCl** (50  $\mu\text{M}$ ) + DNA ( $5.565 \times 10^{-5}$  M base pairs) aggregates.

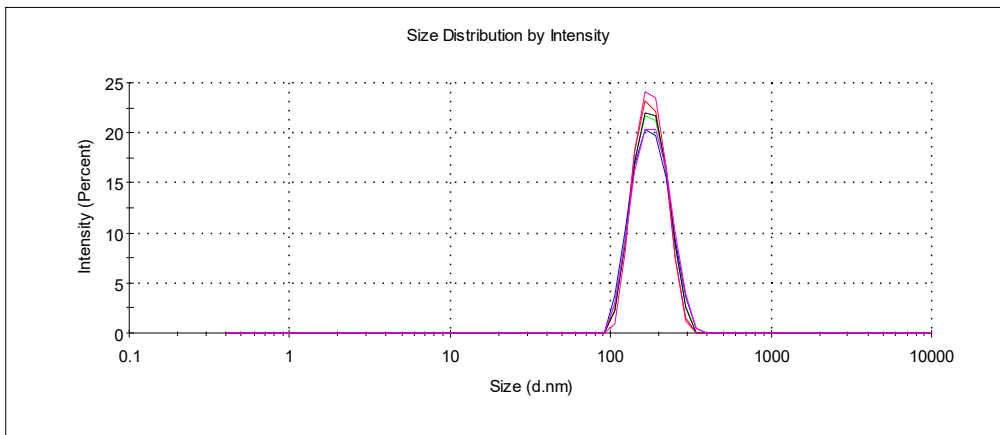


Fig. S63. Size distributions of **G1-cone-HCl** ( $10 \mu\text{M}$ ) + DNA ( $5.565 \times 10^{-5} \text{ M}$  base pairs) aggregates.

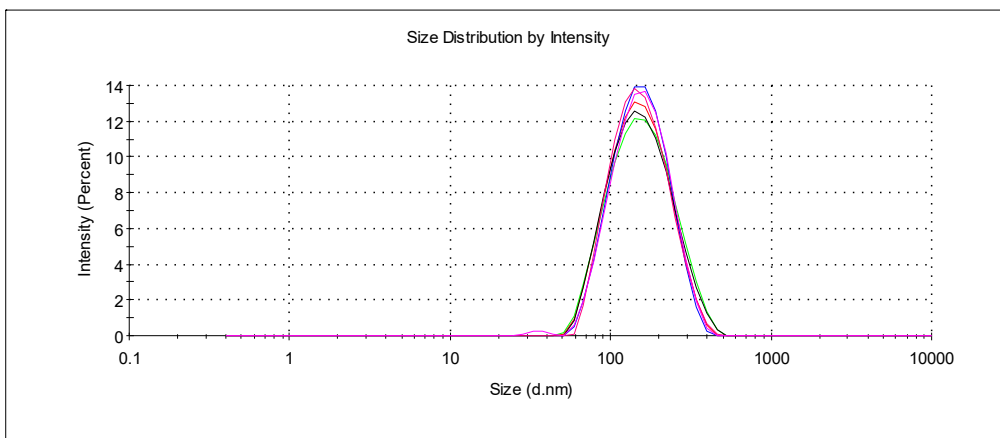


Fig. S64. Size distributions of **G1-cone-HCl** ( $5 \mu\text{M}$ ) + DNA ( $5.565 \times 10^{-5} \text{ M}$  base pairs) aggregates.

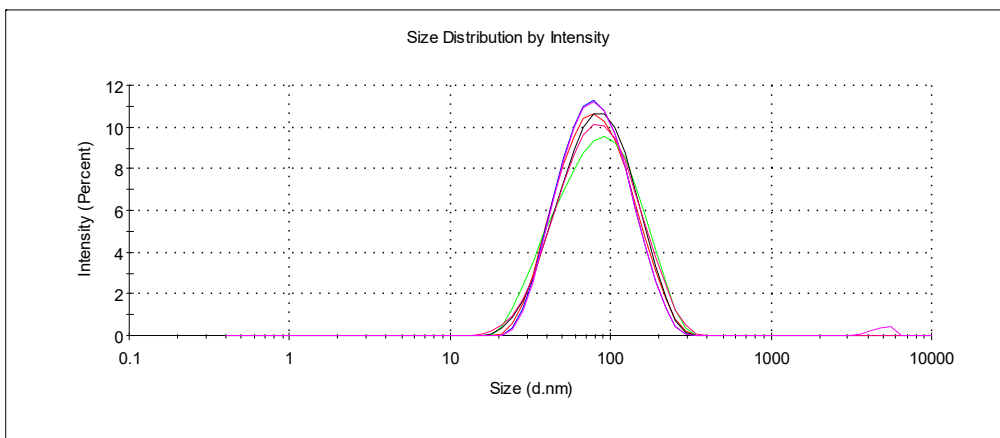


Fig. S65. Size distributions of **G1-paco-HCl** ( $500 \mu\text{M}$ ) + DNA ( $5.565 \times 10^{-5} \text{ M}$  base pairs) aggregates.

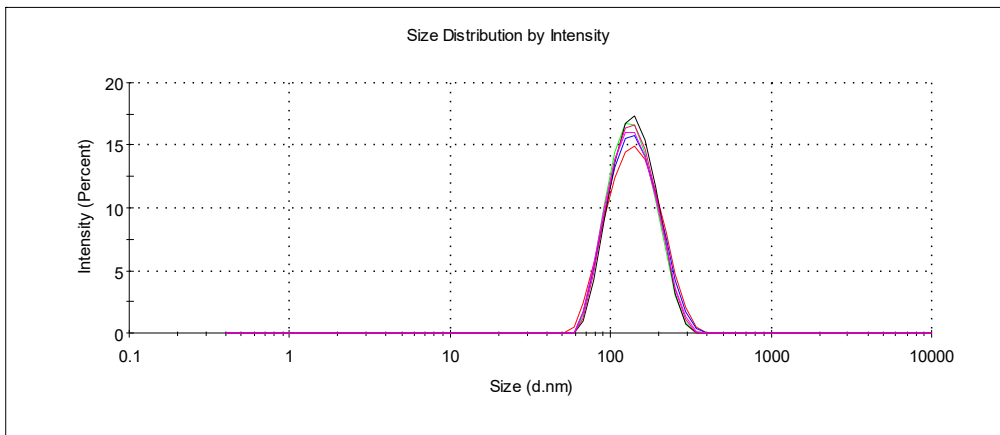


Fig. S66. Size distributions of **G1-paco-HCl** (100  $\mu\text{M}$ ) + DNA ( $5.565 \times 10^{-5}$  M base pairs) aggregates.

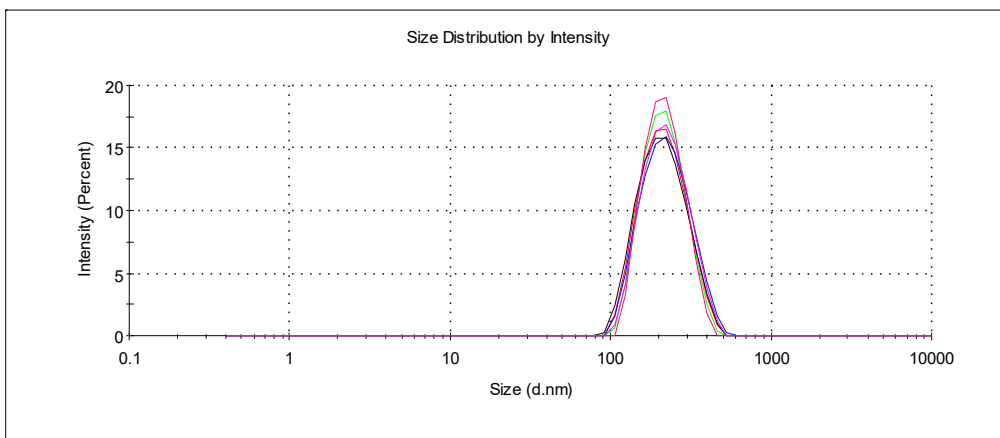


Fig. S67. Size distributions of **G1-paco-HCl** (50  $\mu\text{M}$ ) + DNA ( $5.565 \times 10^{-5}$  M base pairs) aggregates.

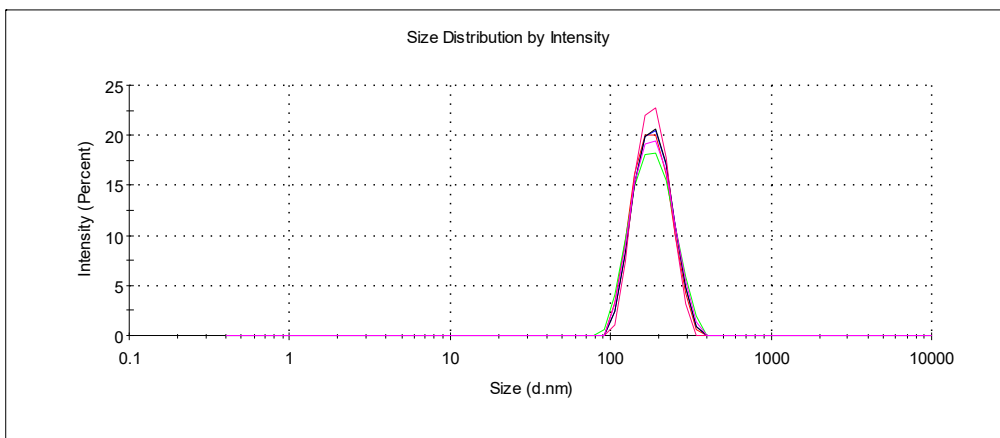


Fig. S68. Size distributions of **G1-paco-HCl** (10  $\mu\text{M}$ ) + DNA ( $5.565 \times 10^{-5}$  M base pairs) aggregates.

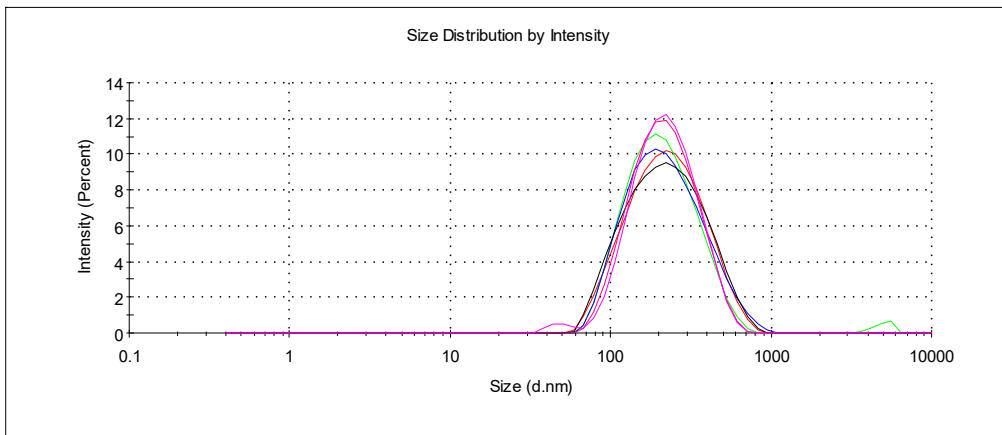


Fig. S69. Size distributions of **G1-paco-HCl** ( $5 \mu\text{M}$ ) + DNA ( $5.565 \times 10^{-5} \text{ M}$  base pairs) aggregates.

## 2.5. TEM images

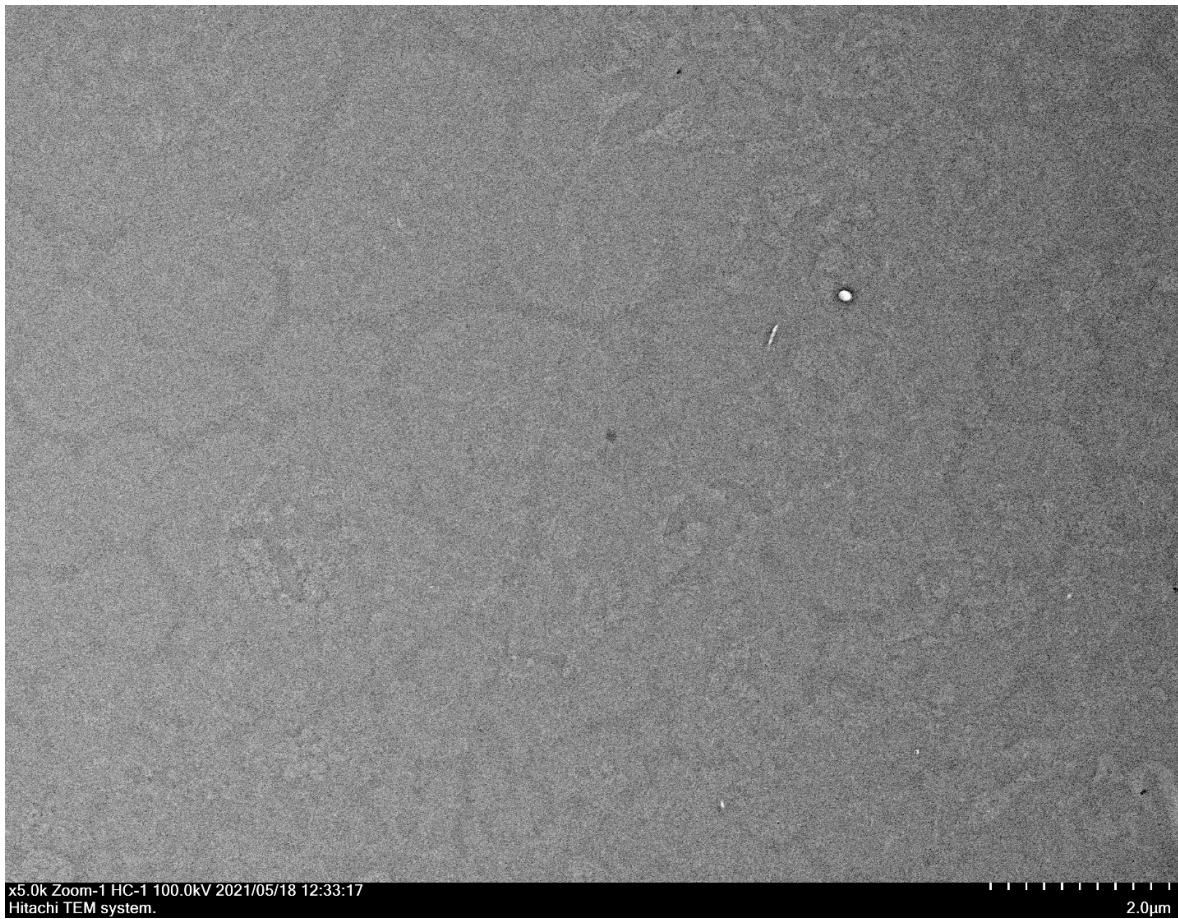


Fig. S70. TEM images of pure **G1-cone-HCl** ( $5 \times 10^{-5}$  M). Scale bar 2  $\mu\text{m}$ .

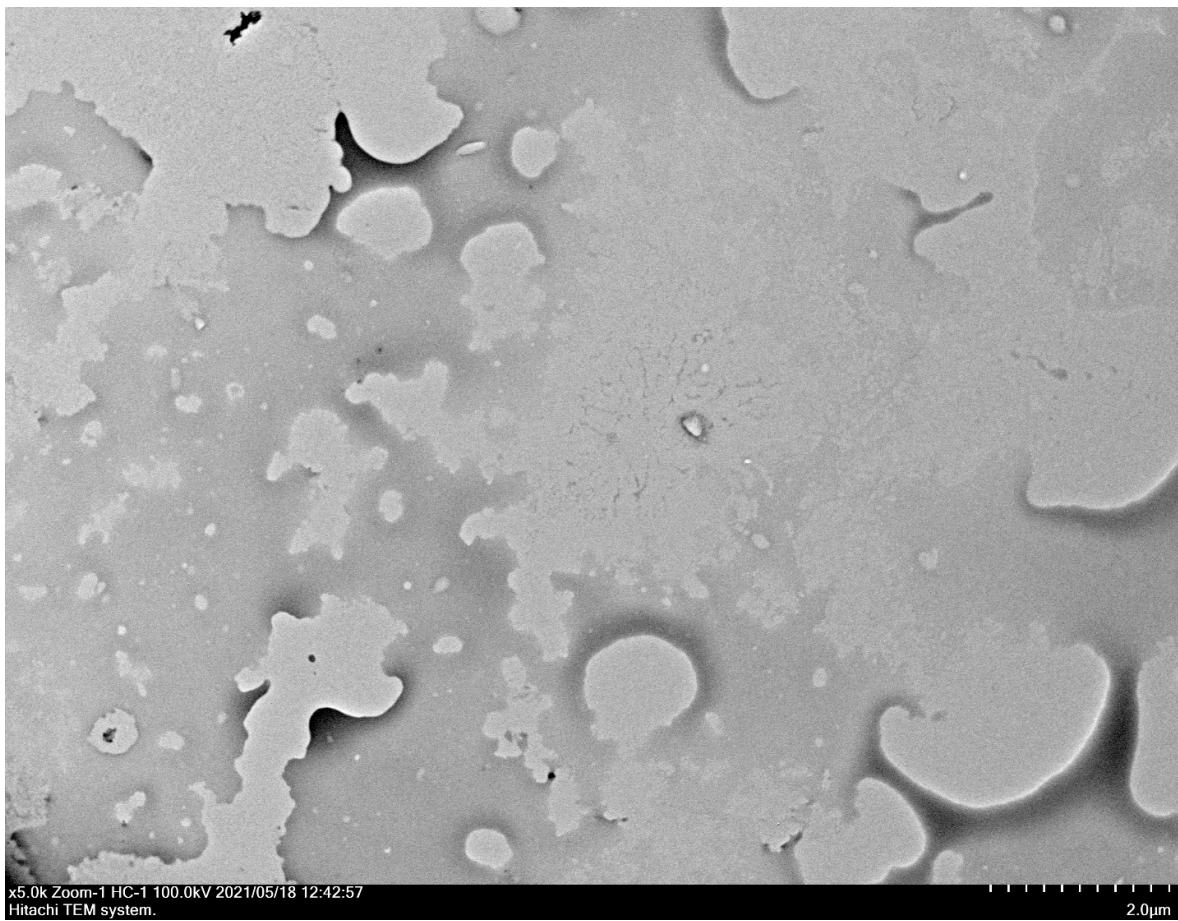


Fig. S71. TEM images of pure DNA ( $5.565 \times 10^5$  M base pairs). Scale bar 2  $\mu$ m.